ASTRONOMY & ASTROPHYSICS
SUPPLEMENT SERIES

Astron. Astrophys. Suppl. Ser. **120,** 229-256 (1996)

Hα emission in pre-main sequence stars. I. An atlas of line profiles*

Bo Reipurth[1], A. Pedrosa[2] and M.T.V.T. Lago[2,3]

[1] European Southern Observatory, Casilla 19001, Santiago 19, Chile
[2] Centro de Astrofísica da Universidade do Porto, Rua do Campo Alegre 823, 4150 Porto, Portugal
[3] Grupo da Matemática Aplicada, Universidade do Porto, Rua das Taipas 135, 4050 Porto, Portugal

Received February 21; accepted April 16, 1996

Abstract. — We present an atlas of very high resolution ($R \sim 50000$) Hα line profiles of 63 pre-main sequence stars, divided among 43 T Tauri stars, 18 Herbig Ae/Be stars, and 2 FU Orionis objects. Hα emission is the most common and prominent spectroscopic feature of pre-main sequence stars, and although it is optically very thick it is still the most frequently modelled emission line in young stars. In T Tauri stars the principal models involve magnetically driven winds, and more recently the role of infalling magnetospheric material has been explored. For Herbig Ae/Be stars a variety of models have been proposed, current emphasis is directed towards obscuration by clumpy circumstellar disk structures. In order to provide constraints on such models, we have made a statistical analysis of the 63 high resolution profiles. We here ignore the considerable variability of the Hα emission, which is discussed in detail in a second paper. Most of our observed lines show complex profiles due to an interplay between emission and absorption features, and we suggest a two-dimensional classification scheme to describe these line profiles, based on the relative height of a secondary peak to the primary peak, as well as whether the absorption is blue- or red-shifted. Among T Tauri stars, 25% have symmetric profiles, 49% have blueshifted absorption dips, and 5% have P Cygni profiles; the remaining 21% show a variety of redshifted absorptions. For Herbig Ae/Be stars symmetric lines are quite rare (11%), indeed almost all of these stars have deep and prominent central absorptions. We have measured the extent of the line wings for all of our stars at the $I_{max}/40$ level, and find that almost all have very extended wings, with typical extents of ±350 km/s, but in high S/N spectra the wings can be traced to lower intensities, and velocities as high as ±900 km/s have been observed. Pronounced asymmetries of these extended wings are found for many stars, suggesting the possibility that the highest velocity material could be non-uniformly distributed. The equivalent widths of the Hα emission in our sample of stars span two orders of magnitude, with a distribution that increases with decreasing equivalent width.

Key words: line: profiles — atlases — circumstellar matter — stars: emission-line — stars: pre-main sequence

1. Introduction

Among the earliest recognized characteristics of young stars in dark clouds was the often strong Hα emission line seen in low dispersion spectra (Joy 1945), and Hα emission remains a prominent feature of almost all known young stars. Indeed, until recently the principal method for identifying new young stars was to perform red objective prism surveys looking for stars with Hα emission near dark clouds.

Herbig (1962) noted that Balmer lines of T Tauri stars can display blueshifted absorption components, and suggested that they are evidence for strong stellar winds, an interpretation that still stands today. Walker (1972) drew attention to a sub-class of the T Tauri stars, the YY Orionis stars, which have redshifted absorption in the Balmer lines, particularly the higher ones. These inverse P Cygni profiles have generally been interpreted in terms of material accreting onto the young stars.

Studies of high resolution emission line profiles offer the possibility to understand the physical conditions in the line-emitting regions. The Hα line has the important advantage for high resolution work that it is usually bright and indeed normally the brightest emission line in a young star. Additionally, it is located at a wavelength near the peak sensitivity of CCD detectors, allowing observations of relatively faint stars even with medium-size telescopes. For these practical reasons, the Hα line is the most commonly observed emission line, and a number of high

Send offprint requests to: Bo Reipurth (reipurth@eso.org)
*Based on observations collected at the European Southern Observatory, La Silla, Chile

resolution studies of Hα emission in T Tauri stars have been made, among others by Hartmann (1982), Mundt (1984) and Fernandez et al. (1995); for Herbig Ae/Be stars Finkenzeller & Mundt (1984) presented a large atlas of Hα profiles. However, the Hα line suffers the drawback that it is usually optically thick, limiting its usefulness as a probe of physical conditions. A more complete understanding of a variety of line-forming regions requires the simultaneous study of the profiles of many lines, and such studies are increasingly becoming available (e.g. Finkenzeller & Basri 1987; Hamann & Persson 1992; Edwards et al. 1994). Nonetheless, within its limitations, the Hα line remains an important probe of circumstellar gas near young stars.

T Tauri stars and Herbig Ae/Be stars differ among other things in their temperatures and amount of UV radiation, and consequently their environments are sufficiently different that we in the following treat these two categories of stars separately. While the Hα line in T Tauri stars is principally shaped by winds and infall, the profile of the Hα line in Herbig Ae/Be stars may be significantly affected by a clumpy circumstellar environment.

In this paper we present high resolution, good signal-to-noise spectra of the Hα line in 63 young, mostly southern stars. The majority are T Tauri stars, but a significant number of Herbig Ae/Be stars were also observed. Fernández et al. (1995) recently presented an atlas of Hα profiles of a similar sized sample of mostly northern stars; our studies have only 6 stars in common, and therefore largely complement each other. The purpose of the present study is to analyze statistically the properties and profiles of the Hα line in a large sample of pre-main sequence stars. Many of the stars have been observed more than once, on time-scales of weeks and years, and we discuss the variability of the Hα line in a subsequent paper (Pedrosa et al. 1997, hereafter Paper II).

2. Observations

The observations were carried out at the La Silla Observatory (ESO) with the 1.4 m Coudé Auxiliary Telescope (CAT) and the Coudé Echelle Spectrograph (CES). We used the short camera mode and a high resolution detector, CCD (ESO #9) with 640×1024 pixels of 15× 15μm size, yielding a resolving power $\frac{\lambda}{\Delta\lambda} = 55000$. Details of the instrument are given by Lindgren & Gilliotte (1989). The relatively long integration times allowed us to achieve good S/N, typically between 10 and 100, and each spectrum covers approximately 50 Å centered at Hα. To calibrate the spectra in wavelength, one exposure of the thorium lamp was done after each exposure of the stars while for the flat-field calibration we used a screen installed at the dome.

The present spectra were obtained with an identical instrumental configuration in five different runs: May/June 1987, December 1987/January 1988, August 1990, February 1993, and March 1994. This set of data covers the majority of southern young stars with Hα emission that can be observed with this telescope, considering the relatively low efficiency of the CES, the resolution and the telescope size, therefore restricting the observations to stars brighter than $V = 12-13$. Consequently our program was limited by the scarcity of bright stars and the relatively long integration times needed to achieve such a relevant S/N ratio while looking at the detailed shape of the Hα line profile.

We have observed 63 young stars, and have obtained a total of 219 spectra, of which we here show one per star. Time series of spectra for selected stars will be discussed in Paper II. Approximately three quarters are T Tauri stars and the remaining are Ae/Be stars. Table 1 presents a list of the stars along with other useful information. The first column gives the most common name for each star, the second column lists the HBC number from Herbig & Bell (1988), the third column adds other common names, the fourth column gives the 1950 position, followed in the fifth column by a spectral type, mostly taken from Herbig & Bell (1988). The sixth column lists a representative V-magnitude, but it should be kept in mind that almost all these stars are likely to be variable. The seventh column gives the equivalent width of Hα corresponding to the line profile shown in Fig. 1. The eight column lists the heliocentric velocity of the star which we have used to indicate the rest velocity of each star in Fig. 1; a colon indicates that the velocity is uncertain, either because it is a mean of velocities for surrounding stars in the same association, or it is the velocity of the associated molecular cloud. The ninth column gives the velocities of the blue and red emission line wings at 1/40 of the observed peak intensity, relative to the stellar rest velocity, that is, the wavelengths of the $I_{\max}/40$ points have been converted to velocity after adjusting for the stellar velocity listed in column seven. The tenth column gives our classification of the Hα profile, and the last column indicates the date on which the spectrum of each star in Fig. 1 was taken.

The data was reduced using MIDAS routines, at La Silla and at the Centro de Astrofísica da Universidade do Porto. Procedures were developed for automatic reduction following the usual steps, namely,

- evaluation of the average bias level
- subtraction to the calibration and flat field frames
- flat-fielding
- sky subtraction
- spectra extraction
- line identification
- wavelength calibration.

The bias frames were not subtracted to avoid the introduction of an extra source of noise. The analysis of dark frames or even the CCD pixels not exposed, showed that there was no need for dark subtraction even for the longer exposures.

Table 1. Pre-main sequence stars observed

Star	HBC	other identification	α (1950)	δ (1950)	Spec. type	V [mag]	W_{eq} [Å]	V_{Hel} [km/s]	$V(I_{max}/40)$ [km/s]	Hα Type	Date
T Tau	35		4 19 04.2	19 25 05	K0	9.9	71.8	+19	−318, +326	III B	14 Aug 90
UX Tau A	43		4 27 10.0	18 07 21	K2	10.7	6.2	+14	−304, +272	II R	1 Jan 88
GG Tau	54		4 29 37.1	17 25 22	K7	12.2	31.2	+18	−296, +284	III B	2 Jan 88
UX Ori	430		5 02 00.6	−03 51 20	A3	9.7	5.4	+26:	−453, +331	III Rm	24 Feb 93
CO Ori	84		5 24 51.2	11 23 12	F8	9.8	4.2	+23	−21, +363	IV Bm	2 Jan 88
GW Ori	85		5 26 20.8	11 49 53	G5	9.8	29.2	+25var	−337, +362	I	28 Dec 87
HK Ori	94		5 28 40.1	12 07 00	A	11.6	40.2	+26:	−316, +280	II B	1 Jan 88
V1044 Ori	113		5 31 49.3	−05 38 44	G5	11.5	4.0	+26	−261, +275	II Bm	22 Feb 93
EZ Ori	114		5 31 50.8	−05 06 46	G0	11.6	11.7	+26:	−323, +257	III Bm	15 Aug 90
LL Ori	126		5 32 38.2	−05 27 14	K2,3	11.7	42.5	+27	−290, +313	III B	25 Feb 93
V380 Ori	164		5 33 59.5	−06 44 46	A1:	10.0	94.2	+22	−269, +284	I	13 Mar 94
P2441	167		5 34 22.7	−04 27 27	G5:	10.8	12.9	+29	−167, +253	IV B	12 Mar 94
V586 Ori	485		5 34 32.7	−06 11 02	A2	9.5	12.4	+26:	−364, +323	II Rm	26 Feb 93
BF Ori	169		5 34 47.2	−06 36 45	A5	10.3	11.3	+26:	−355, +442	III Rm	25 Feb 93
FU Ori	186		5 42 38.0	09 03 02	FUor	9.2	1.4	+28	−26, +243	IV B	29 Dec 87
R Mon	207		6 36 26.0	08 46 54	B	11.3	47.0	+27	−480, +557	III B	1 Jan 88
Z CMa	243		7 01 22.5	−11 28 36	FUor	9.3	20.9	+30	−120, +353	IV B	28 Dec 87
NX Pup	552	CoD −44°3318, Bs 135	7 17 56.5	−44 29 35	F1:	9.8	48.3	+17	−382, +408	II B	29 Dec 87
ESO Hα 28			8 33 33.6	−40 26 11	B8	12.3	51.3	+20:	−314, +362	II Bm	1 Jan 88
ESO Hα 137			8 38 34.0	−40 53 30	B3	12.1	28.0	+21:	−286, +310	I	2 Jan 88
HD 76534			8 53 20.6	−43 16 30	B2	8.2	10.6	+17	−325, +312	II B	24 Feb 93
SY Cha	565	Sz 3, HM 7	10 55 18.5	−76 55 35	M0:	13.0	23.8	+15	−264, +191	I	22 Feb 93
SZ Cha	566		10 57 05.7	−77 01 17	K0	12.0	3.5	+14	−272, +272	III Rm	22 Feb 93
CR Cha	244	Sz 6, LHα 332-20, HM 4	10 57 50.8	−76 45 33	K2	11.2	29.5	+14	−281, +267	I	1 Jun 87
TW Hya	568		10 59 30.1	−34 26 07	K7	10.9	194.	+12	−332, +287	III B	22 Feb 93
CS Cha	569	Sz 9, HM 7	11 01 07.8	−77 17 25	K5:	11.6	54.3	+15	−318, +234	II B	26 Feb 93
CT Cha	570	Sz 11, HM 9	11 02 43.6	−76 11 06	K7:	12.4	65.6	+14	−369, +364	II Rm	4 Jun 87
DI Cha	245	Sz 19, HM 13, LHα 332-17	11 05 57.5	−77 21 50	G2	10.7	16.6	+13	−243, +250	III B	30 May 87
VW Cha	575	Sz 24, HM 17	11 06 38.1	−77 26 12	K2	12.5	71.7	+21	−402, +428	III B	1 Jun 87
CU Cha	246	HD 97048, Sz 25, HM 18	11 06 39.6	−79 23 01	A0p	8.4	48.7	+26:	−233, +312	IV Bm	24 Feb 93
CoD −29°8887			11 06 48.8	−29 45 23	M0	11.1	1.8	+10	−100, +83	I	25 Feb 93
VZ Cha	578	Sz 31, HM 22	11 07 51.9	−76 07 02	K6	12.8	58.2	+14	−334, +353	I	26 Feb 93
Hen 3-600			11 08 05.5	−37 15 33	M3	12.1	30.8	+12	−240, +160	Im	24 Feb 93
WW Cha	580	Sz 34, HM 24	11 08 28.5	−76 18 38	K5:	13.3	65.8	+6	−401, +520	III Bm	24 Feb 93
Sz 41	588		11 10 50.2	−76 20 45	K0	11.6	1.4	+16	−237, +251	I	23 Feb 93
CV Cha	247	Sz 42, HM 30, LHα 332-21	11 10 53.8	−76 28 01	G8	11.0	70.7	+13	−407, +305	II B	9 Mar 94
BF Cha		Sz 54	13 01 24.6	−77 22 57	?	12.5	43.0	+14:	−326, +329	III B	27 Feb 93
HT Lup	248	Sz 68, CoD −33°10685	15 42 01.4	−34 08 08	K2	10.3	7.3	−2	−284, +282	II Bm	23 Feb 93
GQ Lup	250	Sz 75, CoD −35°10525	15 45 58.3	−35 29 58	K7	11.4	31.7	−4	−403, +300	II R	31 May 87
Sz 77	603		15 48 32.4	−35 47 47	M0	12.5	9.4	−3	−196, +192	Im	4 Jun 87
Sz 82	605		15 52 51.1	−37 47 24	M0	11.9	4.7	−3	−180, +119	IV Rm	4 Jun 87
RU Lup	251	Sz 83	15 53 24.3	−37 40 35	K	10.5	136.	−1	−386, +395	II Rm	16 Aug 90
RY Lup	252		15 56 05.0	−40 13 36	K0,1	10.4	7.3	−4	−286, +265	III Bm	1 Jun 87
EX Lup	253	HD 325367	15 59 42.6	−40 10 09	M0:	13.1	31.3	−4	−381, +279	II B	13 Mar 94
HO Lup	612	Sz 88	16 03 39.4	−38 54 19	M1	12.9	239.	−3:	−384, +358	II B	4 Jun 87
HK Lup	616	Sz 98	16 05 00.9	−38 56 44	K7,M0	12.9	41.8	−1	−380, +290	II Bm	1 Jun 87
HR 5999	619	V856 Sco, HD 144668	16 05 12.8	−38 58 23	A7	6.8	10.0	−3:	−377, +345	II B	16 Aug 90
ESO Hα 300			16 05 11.7	−38 58 11:	?	13:	14.0	−4:	−261, +280	I	1 Jun 87
AS 205	254		16 08 37.7	−18 30 43	K5	12.4	103.	−25	−422, +443	III Bm	26 Feb 93
AS 206	259	SR 4, DoAr 20, ROX 6	16 22 54.9	−24 14 02	K6,7	12.9	100.	−5	−354, +375	II R	16 Aug 90
AS 207	264	SR 9, DoAr 34, ROX 29	16 24 38.9	−24 15 23	K5,7	11.4	6.4	−8	−236, +131	IV Rm	15 Aug 90
Haro 1-16	268	DoAr 44, ROX 44	16 28 31.7	−24 21 10	K2,3	12.6	57.8	−5	−310, +288	II R	15 Aug 90
Elias 2-49		HD 150193, MWC 863	16 37 16.4	−23 47 56	A0	9.1	10.7	−6:	−297, +306	III Bm	26 Feb 93
AS 209	270	V1121 Oph	16 46 25.2	−14 16 56	K5	11.5	94.6	−9	−384, +363	I	5 Jun 87
AK Sco	271	CoD −36°11056	16 51 23.1	−36 48 29	F5	8.8	2.8	−1	−362, +348	II R	15 Aug 90
V4046 Sgr		AS 292, HD 319139	18 10 53.7	−32 48 27	K5,6	10.4	41.9	−7	−283, +313	I	17 Aug 90
VV Ser	282	IrCh 21	18 26 14.3	00 06 40	A2	11.8	46.5	−5:	−426, +460	II B	17 Aug 90
S CrA	286		18 57 46.1	−37 01 37	K6:	11.1	120.	0:	−429, +427	III Bm	4 Jun 87
R CrA	288		18 58 31.6	−37 01 30	A5:	10.7	102.	0:	−396, +353	II R	30 May 87
T CrA	290		18 58 36.5	−37 02 10	F0:	13.4	18.6	0:	−351, +350	II R	16 Aug 90
VV CrA	291		18 59 43.9	−37 17 15	K7:	13.0	35.4	0:	−222, +315	III Bm	4 Jun 87
AS 353A	292	V1352 Aql, IrCh 34	19 18 09.4	10 56 15	K2	12.5	86.6	−15:	−568, +654	III B	5 Jun 87
WW Vul	686	BD+20°4136, HD 344361	19 23 49.0	21 06 28	A0,3	10.6	17.9	−18:	−391, +399	II B	22 Aug 90

For the sky subtraction we used two pairs of columns at each side of the spectra. In the case of the LL Ori spectra we can still see the Orion Nebula emission lines of N[II] (6548 Å, 6584 Å) and Hα superimposed on the stellar spectra, presumably due to inhomogeneities in the Orion Nebula. By comparison with spectra where this contribution was not removed we conclude that the procedure used was able to remove 99% of the sky background. The same phenomena could be observed in V1044 Ori but due to the lower contribution from the Orion Nebula, the residual effect is undetectable.

Any remaining error in the wavelength calibration is expected to be smaller than 0.003 Å (0.14 km s^{-1}). The spectra were normalized to the continuum. It was obtained by fitting a spline to points selected with the cursor away from the Hα line. The final spectra were calibrated to heliocentric velocities.

3. The atlas

In Fig. 1 we show 63 panels with an Hα emission line profile for each of the stars we have observed. The date of observation is indicated in Table 1. Each panel indicates with a horizontal dotted line the continuum, normalized to a value of 1.0. A vertical dotted line is shown at the stellar heliocentric velocity listed in Table 1. A second horizontal dotted line is plotted above, at 1/40 of the observed peak emission; the velocities where the blue and red wings cut this line are listed in Table 1. For each panel is given the

name of the star, its emission line class (see Sect. 7) and its type (T: T Tauri star, H: Herbig Ae/Be star, F: FUor).

The heliocentric velocities for the stars have been taken from the literature. In the cases where no velocity could be found, either a velocity of the associated CO gas or a mean of surrounding stellar velocities was used; such velocities are marked with a colon.

We note that very broad low level features, like underlying weak and broad photospheric absorption lines seen in a few Herbig Ae/Be stars, are likely to be removed in the normalization process, since the wavelength range of the echelle order containing Hα is small.

3.1. *Stellar absorption lines*

It is common for T Tauri stars to show a great number of photospheric absorption lines, and they are visible in many of the spectra presented here, although they change according to the spectral type and in some cases they are diluted by the veiling. For a detailed line identification the spectrum of an unveiled WTTS CoD −29° 8887, of spectral type M0, is shown in Fig. 2 with the stronger lines labelled with their rest wavelengths according to Moore (1972). Any difference in wavelength between this spectrum and the ones in the atlas is due to the different stellar radial velocities.

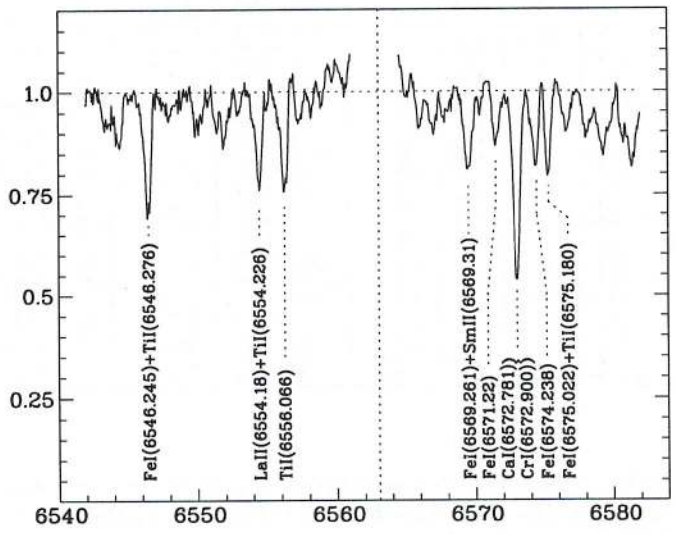

Fig. 2. Photospheric lines of an M0 star (CoD −29°8887

3.2. *Atmospheric H_2O lines*

The spectra usually show very narrow absorption lines due to water vapor. They are stronger for those spectra obtained in the runs of May/June 1987 and March 1994. The lines are variable, not only in strengh but their ratios can also vary, as seen for example by comparing the absorptions present in the blue part of the continuum of RY Lup and DI Cha.

In Fig. 3 we show a spectrum obtained from normalizing a stellar spectrum with Hα in absorption. It is labeled with the wavelengths taken from the solar spectrum of Moore et al. (1966).

The reader should keep in mind when comparing this spectrum with the atlas, that the wavelengths of the absorptions change according to the heliocentric correction applied to each spectrum. It should be noted that there are several H_2O lines that fall near the peak of the Hα emission in many of the spectra shown here, particularly clear examples are seen in VW Cha, CV Cha and S CrA. However, they do not significantly affect the Hα line profile, because they are comparatively much narrower and weaker.

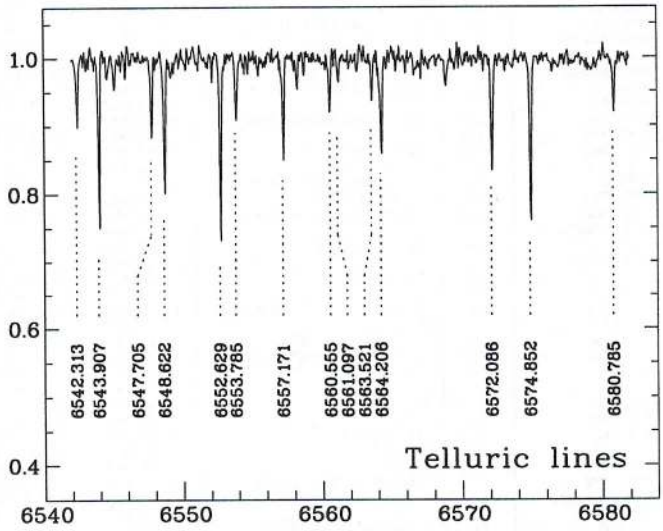

Fig. 3. Telluric absorption lines obtained from normalization of an early-type stellar spectrum with Hα in absorption

4. Comments on individual stars

T Tau. A classical T Tauri star with a strong emission line spectrum, and prototype of its class. Hα profiles are shown by Hartmann (1982) and Mundt (1984). It has a bright infrared companion (e.g. Maihara & Kataza 1991), and both drive Herbig-Haro flows (e.g. Böhm & Solf 1994).

UX Tau-A. A weak-line T Tauri star, which is part of a triple system (e.g. Reipurth & Zinnecker 1993; Magazzú et al. 1991).

GG Tau. A classical T Tauri star, which is part of a hierarchical quadruple system (Leinert et al. 1991). An extended disk structure is resolved around the star (e.g. Kawabe et al. 1993; Dutrey et al. 1994). Spectroscopic studies by e.g. Hartigan et al. (1991) and Valenti et al. (1993).

UX Ori. A Herbig Ae/Be star with the spectroscopic and infrared properties of its class, but not associated with nebulosity. The star is highly variable, with occasional

deep minima of 2−3 mag in V. A number of photometric studies have been made (e.g. Evans et al. 1989; Bibo & Thé 1990, 1991; Herbst et al. 1994), and a detailed spectroscopic/photometric study is presented by Grinin et al. (1994), including high-resolution spectra of the Hα line.

CO Ori. A T Tauri star; with a spectral type between F8 and G5, this is one of the more luminous T Tauri stars known. The star is a visual binary (Herbig 1962; Reipurth & Zinnecker 1993). Photometric variations are discussed by Herbst et al. (1994). An Hα profile is shown by Fernández et al. (1995). It is noteworthy that the Hα profile is reminiscent of FU Ori with a pronounced P Cygni profile, and combined with the early spectral type (for a T Tauri star) and its brightness, this could suggest that CO Ori is a star gradually coming out of a FUor outburst.

GW Ori. A classical T Tauri star; with a spectral type of G5 this is one of the more luminous members of the class. An Hα profile is shown by Hartmann (1982) and Fernández et al. (1995). It is a spectroscopic binary (Mathieu et al. 1991), surrounded by significant amounts of circumbinary material (Mathieu et al. 1995).

HK Ori. A Herbig Ae/Be star. Spectral and photometric characteristics are discussed by Herbig (1960). Its emission line spectrum is studied by Hamann & Persson (1992) and Böhm & Catala (1994). An Hα profile is shown by Finkenzeller & Mundt (1984). It is associated with a Herbig-Haro object (Goodrich 1993).

V1044 Ori. A little studied rather luminous T Tauri star. The apparent P Cygni profile seen in Fig. 1 is caused by the presence of a wide stellar absorption line, probably broadened by very large rotation.

EZ Ori. A little studied T Tauri star.

LL Ori. A little studied T Tauri star. It is located in a bright and very inhomogeneous part of the Orion Nebula, which makes extraction of an Hα line profile difficult.

V380 Ori. A Herbig Ae/Be star. Herbig (1960) gives a detailed spectral description. A companion with a separation of 0.17 arcsec was found by Leinert et al. (1994). An Hα profile is shown by Garrison & Anderson (1977) and Finkenzeller & Mundt (1984). The star drives several HH objects (Herbig 1974; Corcoran & Ray 1995) and a molecular outflow (Levreault 1988).

P2441. A G-type star with Hα emission and Li absorption, belonging to the Orion association (Cohen & Kuhi 1979; King 1993). It is a visual binary and is associated with Herbig-Haro objects (Reipurth & Graham 1988).

V586 Ori. A Herbig Ae/Be star according to Thé et al. (1994). Photometry is presented by Pugach & Kovalchuk (1986) and Bibo & Thé (1991).

BF Ori. A Herbig Ae/Be star, which has been extensively observed. Photometric variability is discussed by Bibo & Thé (1991) and a detailed spectroscopic study is presented by Welty et al. (1992a). An Hα profile is shown by Finkenzeller & Mundt (1984).

FU Ori. An FU Orionis star, and prototype of its class. The photometric and spectral evolution is discussed by Herbig (1966, 1977). A vast literature exists on this star. A number of theoretical models for line formation exists; a recent one, with references to the literature, is Hartmann & Calvet (1995).

R Mon. A Herbig Ae/Be star. The star and its environment is very well studied at all wavelengths. A detailed spectroscopic analysis is made by Herbig (1968). An Hα profile is shown by Finkenzeller & Mundt (1984). The star is surrounded by a disk (Sargent & Beckwith 1987), a large variable reflection nebula (e.g. Lightfoot 1989), and drives Herbig-Haro objects (e.g. Schwartz & Schultz 1992).

Z CMa. An FU Orionis star (Hartmann et al. 1989), which is very well studied at all wavelengths. The photometric history is summarized by Covino et al. (1984). High resolution spectroscopy is presented by Finkenzeller & Mundt (1984), and modelled by Welty et al. (1992b). The evolutionary state of the star is considered by Hessman et al. (1991). The star has an infrared companion, (e.g. Koresko et al. 1991), and the system drives a Herbig-Haro jet (Poetzel et al. 1989).

NX Pup. A Herbig Ae/Be star (Tjin-A-Djie et al. 1984). The photometric behaviour is discussed by Bibo & Thé (1991). An Hα profile is shown by Finkenzeller & Mundt (1984). The star is located in a Bok globule (Reipurth 1983), and has two companions (Brandner et al. 1995).

ESO-Hα 28. An Hα-emission star in RCW27 in the Vela star forming region (Pettersson & Reipurth 1994). Of spectral type B8, it is probably a Herbig Ae/Be star.

ESO-Hα 137. An Hα-emission star in RCW27 in the Vela star forming region (Pettersson & Reipurth 1994). Of spectral type B3, it is probably a Herbig Ae/Be star.

HD 76534. A probable Herbig Ae/Be star, according to Thé et al. (1985, 1994). An Hα profile is shown by Finkenzeller & Mundt (1984). The star is a close visual binary (Innes 1927; Reipurth & Zinnecker 1993).

SY Cha. A little studied T Tauri star (e.g. Gauvin & Strom 1992). There is a weak indication of an inverse P Cygni profile in the spectrum in Fig. 1, but this is not certain, since a group of stellar absorption lines are also present at the same position.

SZ Cha. A little studied T Tauri star (e.g. Gauvin & Strom 1992).

CR Cha. A T Tauri star. High resolution spectroscopy is discussed by Finkenzeller & Basri (1987), Hamann & Persson (1992) and Batalha & Basri (1993).

TW Hya. A classical T Tauri star. A spectroscopic and photometric study is presented by Rucinski & Krautter (1983). Further high-resolution spectra are given by Franchini et al. (1992).

CS Cha. A T Tauri star (e.g. Gauvin & Strom 1992).

CT Cha. A T Tauri star. A spectroscopic study is presented by Hamann & Persson (1992).

DI Cha. A T Tauri star. The star has a faint companion (e.g. Reipurth & Zinnecker 1993). High resolution spectroscopy is presented by Finkenzeller & Basri (1987), Franchini et al. (1991, 1992), and Batalha & Basri (1993).

VW Cha. A T Tauri star. High resolution spectroscopy is discussed by Hamann & Persson (1992).

CU Cha. A bright Herbig Ae/Be star, that is particularly well studied in the infrared (see e.g. Assendorp et al. (1990) for references).

CoD−29°8887. A weak-line T Tauri star according to de la Reza et al. (1989). It is a binary (Reipurth & Zinnecker 1993).

VZ Cha. A T Tauri star. Detailed high resolution spectroscopy is presented by Krautter et al. (1990) and Hamann & Persson (1992).

Hen 3-600. A binary T Tauri star, with components of almost equal brightness. Both stars show Hα emission (de la Reza et al. 1989). The separation of the components is 1.″5, and both stars fell in our slit.

WW Cha. A little studied T Tauri star (e.g. Gauvin & Strom 1992).

Sz 41. A little studied T Tauri star (e.g. Gauvin & Strom 1992). The star is a binary (Reipurth & Zinnecker 1993).

CV Cha. A T Tauri star. High resolution spectroscopy is presented by Penston & Lago (1983), Appenzeller & Wagner (1989) and Hamann & Persson (1992). The star is a binary (e.g Reipurth & Zinnecker 1993).

BF Cha. A little studied T Tauri star (e.g. Gauvin & Strom 1992).

HT Lup. A weak line T Tauri star. High resolution spectroscopy is discussed by Finkenzeller & Basri (1987), Hamann & Persson (1992), Franchini et al. (1992) and Batalha & Basri (1993). The star has a companion (Reipurth & Zinnecker 1993), and the system drives a Herbig-Haro jet (Heyer & Graham 1989).

GQ Lup. A T Tauri star (e.g. Hughes et al. 1994). High resolution spectroscopy is discussed by Appenzeller et al. (1978), Bertout et al. (1982), Appenzeller & Wagner (1989) and Hamann & Persson (1992)

Sz 77. A T Tauri star (e.g. Hughes et al. 1994). High resolution spectroscopy is discussed by Finkenzeller & Basri (1987) and Batalha & Basri (1993)

Sz 82. A T Tauri star (e.g. Hughes et al. 1994). High resolution spectroscopy is discussed by Finkenzeller & Basri (1987) and Batalha & Basri (1993)

RU Lup. A T Tauri star. High resolution spectroscopy is discussed by Schwartz & Heuermann (1981), Lago (1982), Hamann & Persson (1992), Hamann (1994) and Giovanelli et al. (1995). Photometric variations are discussed by e.g. Hutchinson et al. (1989) and Giovanelli et al. (1991).

RY Lup. A T Tauri star. Photometric variations are discussed by e.g. Liseau et al. (1987), Gahm et al. (1989) and Hutchinson et al. (1989). Simultaneous spectroscopic and photometric observations are presented by Gahm et al. (1993).

EX Lup. A T Tauri star, belonging to the EXor group of eruptive variables (e.g. Herbig 1989). Long term photometry is reported by Bateson et al. (1990). Photometric and spectroscopic observations are discussed by Lehmann et al. (1995).

HO Lup. A little studied T Tauri star (e.g. Hughes et al. 1994). The star is a binary (Reipurth & Zinnecker 1993).

HK Lup. A T Tauri star (e.g. Hughes et al. 1994). High resolution spectroscopy is presented by Finkenzeller & Basri (1987) and Batalha & Basri (1993)

HR 5999. A Herbig Ae/Be star, well studied by many authors. High resolution spectroscopy is presented by Tjin-A-Djie et al. (1989). Monitoring of line profiles is reported by Baade & Stahl (1989). Photometric variability is discussed by Bibo & Thé (1991) and Perez et al. (1992).

ESO-Hα 300. This is a faint star, which is located about 15 to 18 arcsec north-west of HR 5999, the northern star in the bright HR 5999/6000 double. It has been missed in previous Hα surveys (e.g. Schwartz 1977), presumably due to being drowned in the glare of HR 5999, and was observed by us out of curiosity because of its proximity to HR 5999. Upon detection of Hα emission, we here designate it ESO-Hα 300, in the series of ESO-Hα discoveries started by Pettersson & Reipurth (1994). HR 5999 has a companion, Rossiter 3930, of similar brightness to ESO-Hα 300, but in position angle 110° and only 1.3 arcsec from the bright star. These two companions were at some early stage confused, and the Hα spectrum referred to by Stecklum et al. (1995) in fact refer to ESO-Hα 300 and not to Rossiter 3930. No spectral type is known, but our detection of Hα emission strongly suggests that the star is a T Tauri star, similar to the small cluster of Hα emission stars in its immediate surroundings (Schwartz 1977).

AS 205. A T Tauri star (Cohen & Kuhi 1979). An Hα profile is shown by Mundt (1984) and Fernández et al. (1995). High resolution spectroscopy is presented by Hamann & Persson (1992), and Hamann (1994). The star is a binary (Cohen & Kuhi 1979).

AS 206. A T Tauri star. Spectroscopy reported by Bouvier & Appenzeller (1992) and Valenti et al. (1993).

AS 207. A T Tauri star. Spectroscopy reported by Bouvier & Appenzeller (1992) and Valenti et al. (1993).

Haro 1-16. A T Tauri star (Cohen & Kuhi 1979). Spectroscopy reported by Valenti et al. (1993).

Elias 2-49. Probably a Herbig Ae/Be star. It is a bright near-infrared source (Elias 1978). The star is a binary (Reipurth & Zinnecker 1993).

AS 209. A T Tauri star (Cohen & Kuhi 1979). Spectroscopy reported by Valenti et al. (1993). An Hα profile is shown by Fernández et al. (1995).

AK Sco. A Herbig Ae/Be star. Andersen et al. (1989) have made a detailed study, and find that it is a spectroscopic binary. Photometric variability is studied by Bibo & Thé (1991).

V4046 Sgr. An isolated T Tauri star that is a spectrocopic binary (de la Reza et al. 1986, Byrne 1986).

VV Ser. A Herbig Ae/Be star (Herbig 1960). Line profiles are discussed by Ulrich & Knapp (1979). A photometric and spectroscopic study is presented by Chavarria et al. (1988). An Hα profile is shown by Finkenzeller & Mundt (1984) and Fernández et al. (1995).

S CrA. A T Tauri star. Detailed spectroscopic studies are presented by Appenzeller & Wolf (1977), Wolf et al. (1977), Bertout et al. (1982) and Hamann & Persson (1992). High resolution spectroscopy is discussed by Appenzeller et al. (1986), Krautter et al. (1990), Graham (1992), and Hamann (1994). Spectroscopic variability is discussed by Edwards (1979) and Mundt (1979). The star is a close binary (e.g. Reipurth & Zinnecker 1993). The system drives a Herbig-Haro flow (Reipurth & Graham 1988).

R CrA. A Herbig Ae/Be star (Herbig 1960). High resolution spectroscopy is discussed by Hamann (1994). The Hα line is highly variable (Graham & Phillips 1987; Graham 1992). The star drives a Herbig-Haro flow (Graham 1993).

T CrA. A Herbig Ae/Be star. Spectroscopic observations are discussed by e.g. Herbig (1960), Bibo et al. (1992) and Graham (1992). An Hα profile is shown by Finkenzeller & Mundt (1984).

VV CrA. A T Tauri star. High resolution spectroscopy is discussed by Appenzeller et al. (1986), and Hamann (1994). The star is a binary (Graham 1992; Reipurth & Zinnecker 1993).

AS 353A. A T Tauri star. Spectroscopic studies are discussed by Böhm & Raga (1987), Eislöffel et al. (1990), Hamann & Persson (1992), Hamann (1994), and Edwards et al. (1994). An Hα profile is shown by Mundt (1984) and Fernández et al. (1995). The star is a binary (e.g. Reipurth & Zinnecker 1993) and the system drives a Herbig-Haro flow (e.g. Herbig & Jones 1983).

WW Vul. A Herbig Ae/Be star. A detailed study is presented by Friedemann et al. (1993).

5. Models of Hα emission in T Tauri stars

The Hα line is the most prominent feature in the visible spectra of T Tauri stars. As we discuss in Sect. 7, the line strength varies from star to star spanning over two orders of magnitude in equivalent width, up to 250 Å or more in the most extreme cases. The line profile takes a variety of shapes, from symmetric to highly asymmetric, displaying one (or more) absorption components mostly in the blue wing and, less commonly, in the red wing. The strength of these absorptions also varies quite widely although only rarely do they reach below the level of the continuum.

The existence of a variety of processes to produce Hα emission make this line not the most ideal diagnostic tool. This is even more so since the line is always optically very thick in T Tauri stars, and therefore requires an adequate treatment of radiative transfer when modelling the profile. A further complication is due to the fact that the line results from contributions of different regions around the star where a large diversity of physical and dynamical conditions may exist. In fact there is increasing evidence that a significant part of the Hα line flux is produced quite close to the star (in a dense chromosphere or boundary layer, depending on the authors) while a much larger region also gives some contribution. The relative importance of the contributions and extent of such regions, while most probably varying from star to star, is not a settled issue.

Even so, fitting of the Hα line profile is still the most commonly used tool when modelling T Tauri stars, and several approaches have been adopted over the last decades.

Thermally driven winds were ruled out more than a decade ago on the grounds that they failed to comply with the observations: in T Tauri stars the Hα line half width may reach up to 500 km s^{-1} or more, and being late type stars there is no way that such high velocities can be explained just by the effect of thermal pressure, even when a large (and unphysical) turbulent velocity component is included. Similarly, rotation broadening is not of much help - T Tauri stars are mostly relatively slow rotators. Other mechanisms have been invoked, such as opacity effects, but they are only minor contributors - observational evidence for the Sun and theoretical modelling for T Tauri stars (Calvet et al. 1984) show that such contributions are unlikely to play a major role as broadening mechanisms.

To overcome the difficulties in explaining the broad Hα lines that are observed, models of magnetically driven winds were proposed - most of them include the presence of a magnetic field and Alfvén waves propagating outwards as the wind driving mechanism. Although the first models did not attempt to fit the Hα line profile (mainly because of the existing limitations in computing power at the time for an adequate treatment of the radiative transfer), higher Balmer lines, assumed to be optically thin, were fitted using observationally constrained values for the density and velocity as function of height above the stellar photosphere (Lago 1979).

A similar model was also used for a more general discussion on the observable consequences of the magnetic field structure to the shape of the line profiles, including the Hα line (DeCampli 1981). Later, also in a similar model, a schematic treatment of wave dissipation was introduced to obtain the temperature structure in the wind

and to compute the Hα line profiles (Hartmann et al. 1982).

A realistic approach in the treatment of radiative transfer (fifteen levels plus continuum for the H atom model while determining the level populations) was taken by Natta et al. (1988). Although adopting an ad-hoc velocity law, their calculations confirm the very high optical thickness of Hα (and also of Hβ) as well as the dominant contribution of the layers close to the star to the flux in the line; another important result is that such winds are likely to be primarily neutral, therefore removing the apparent contradiction in the values of $\dot{M}$ derived from the stellar winds or from the CO outflows (Evans et al. 1987; Levreault 1988).

Again a spherical wind driven by Alfvén waves was adopted by Hartmann & Kenyon (1990) with a postulated velocity law that included a large turbulent velocity, and radiative transfer was calculated considering an eight level H atom. The resulting flux in the Hα line was found to be not very sensitive to the temperature in the range of values imposed to guarantee the Hα line in emission at distances up to 3 R_*. However, the line profiles were found to be sensitive to the velocity field. The computed Hα (and Hβ) profiles were systematically broader and more asymmetric than observed in T Tauri stars (probably a consequence of the large turbulent velocity component). The blue absorption features overlapping the Hα line are also much broader and deeper (well below the continuum) than most observed ones.

A quite different approach was taken by Calvet et al. (1992). Here the wind (a spherically symmetric flow) was assumed to originate in a boundary layer between the slow rotating star and a rapid rotating disk and to flow within a conical aperture whose geometry (opening and inclination angle) were free parameters. Other free parameters included the inclination of the system (star + disk) relative to the line of sight, as well as the inner and outer radii of the disk, and the mass loss $\dot{M}$. The velocity law was the same as in the Hartmann & Kenyon (1990) models. Some of the features observed in the Hα lines of T Tauri stars, such as the central absorption and, to a less extent, the blue shifted absorption could be reproduced by these models. However, the absorption tends to be excessive when compared to the observations. The attempt to reproduce the centrally peaked or triangular profiles, so frequent in T Tauri stars, led the authors to an alternative set of models where a rotational velocity component was included. The resulting profiles display a double peak structure - a relatively rare occurrence in T Tauri stars - and remained broader than the observed ones, and once more with a deep absorption component well below the continuum. Similar features also characterized the computed Hβ and Hγ line profiles.

A further set of models has been proposed by Calvet & Hartmann (1992). This time, instead of a wind there is an isothermal accretion flow down to the star, following a ballistic law. This accretion of material is restricted to an axially symmetric configuration by a dipolar magnetic field, and the flow velocity constrained by a boundary velocity condition immediately above the stellar surface. These models are able to reproduce reasonably well some of the general characteristics of the Hα line profile in T Tauri stars although in most cases displaying an absorption component (redward displaced) not only in the Hα but also in the higher Balmer lines.

Further development of the previous models has recently been presented by the same authors (Hartmann et al. 1994). A dipolar magnetic field controls the free fall of material from a disk onto the star. The infalling gas reaches velocities up to several hundred km s^{-1} above the stellar surface and is then decelerated in a strong shock. The extent of the magnetosphere (inner and outer radii), its temperature and the star's inclination are the main parameters determining the shape and intensity of the profile of the Balmer lines. These profiles are calculated using a two level model for the hydrogen atom and assuming the ionization to be controlled by the balance between recombination to the second level and photoionization. Other parameters introduced are the mass, radius and temperature of the star. The resulting Hα line profiles are asymmetric and with a red displaced absorption that might reach below the continuum level. The model is therefore able to produce inverse P Cygni type profiles. The blueshifted absorption must arise in a wind. However, the authors argue that the *emission* generally arises in the infalling magnetospheric material, and only the blueshifted *absorption* is due to a wind.

Edwards et al. (1994) present for a sample of 15 classical T Tauri stars a set of high resolution profiles (Hα, Hβ, Hγ, Hδ, He I λ 5876 Å and the Na I D lines) with the goal of establishing the percentage of CTT showing evidence for high speed mass infall. The authors adopt the models of Hartmann et al. (1994) and although the sample is too small for a complete statistical analysis they do see evidence that the Balmer emission forms predominantly in infalling zones in most CTT stars.

Models of stochastic winds in which blobs of material are accelerated in the region close to the star and decelerated further out have been proposed by Grinin & Mitskevich (1991) and Mitskevich et al. (1993). The main parameters are the (prescribed) acceleration force and extent of the region where it occurs, before the deceleration of the wind sets in, and a volume filling factor. This last parameter seems to determine whether the resulting Hα profile is double or single peaked. The main difficulties of these models when comparing with the observed Hα profiles are the far too narrow separation between the emission peaks in the case of the double profiles, and the excessive sharpness of the blue side of the main peak emission.

Nevertheless these models propose a natural solution for a wide range of observed Hα line profiles and associated variability. Furthermore, there are other lines of evidence supporting the presence of a wind comprising an acceleration region close to the star, followed by deceleration further out in some TTS (Penston & Lago 1982).

The detailed modelling of line profiles, mainly for the very thick lines such as Hα, is very sensitive to the radiative transfer and the calculation of the level populations, as well as to the density and velocity conditions. Therefore, the adoption of a simplified treatment can lead to misleading results. Furthermore, there is growing evidence that the Hα line might result from the combined contribution of more than one region. Such evidence comes from speckle interferometric observations. In T Tau, as much as 80% of the flux in the Hα line originates in a region only marginally resolved (approx. 0.05″) the remaining 20% resulting from a region of several hundred stellar radii (Devaney et al. 1995). A detailed study of the behaviour of the Hα line profile on various time scales in LkHα 264 also points in the same direction: the highly variable component of the Hα line affects mainly the blue side and the central region of the profile and has to be produced in a relatively narrow and dense region, not too far from the stellar surface (Gameiro & Lago 1995).

6. Models of Hα emission in Herbig Ae/Be stars

Herbig (1960) identified the class of the Ae/Be stars in order to find and study the higher-mass counterparts to the T Tauri stars. In the intervening years, Herbig's Ae/Be stars have been confirmed as pre-main sequence (PMS) stars with masses of about 2 to 10 $M_{\odot}$. From the point of view of the present study, it is important to note that it is not easy in all cases to separate Herbig Be stars from the conventional Be stars (e.g. Herbig 1994), and consequently we cannot be totally certain that each one of the stars listed in Table 1 as Herbig Ae/Be stars are indeed PMS objects.

Finkenzeller & Mundt (1984) made a comprehensive study of Hα profiles of Herbig Ae/Be stars based on high-resolution spectroscopy, and found that 95% of the profiles could be classed as either "double-peaked", "single-peaked" or "P Cygni", with only 5% showing more complex shapes.

Variability of the Hα emission is a characteristic of Herbig Ae/Be stars, and some stars are known to change their Hα profiles from one type to another (e.g. Herbig 1960; Finkenzeller & Mundt 1984; Catala 1994). This is discussed in more detail in Paper II, here we merely note that such profound changes in the Hα emission suggest that the type of Hα emission profile is not linked to different masses or evolutionary status (e.g. Catala 1989).

While the presence of P Cygni profiles at Hα is widely accepted as originating in a stellar wind, the other profiles have been interpreted in a variety of models, outlined below (see also Catala 1994).

Clumpy circumstellar environment

A sub-set of the Herbig Ae/Be stars belong to the photometrically defined group of variable stars with non-periodic Algol-type minima (Hoffmeister 1949), which we here prefer to call stars with deep minima.[1] Four of the Herbig Ae/Be stars we have observed (UX Ori, V586 Ori, BF Ori and WW Vul) belong to this group. A crucial observational fact is that the polarization increases strongly as the star fades, while the colours, after an initial reddening, become bluer again. Grinin (1992) suggests that clumps in a circumstellar disk seen more or less edge-on occasionally obscure the star, making the scattered radiation of the disk account for a larger fraction of the total light, thus increasing the polarization and the blue light. Voshchinnikov et al. (1995) find that up to 30% of the total radiation may be scattered by dust grains. At the same time, the equivalent width of the Hα emission increases (Kolotilov 1977; Herbst et al. 1983), which suggests that the Hα emission arises at least partly in an extended circumstellar gas envelope that is less occulted by the clumps than the star itself. In the case of UX Ori, Grinin et al. (1994) found that Hα changed from an inverse P Cygni profile at light maximum to a symmetrical line at minimum, which has been modelled with the variable screening model by Grinin & Tambovtseva (1995). Further support for this model comes from the fact that Herbig Ae/Be stars with Hα profiles with deep central absorptions are also having larger photometric variations (Grinin & Rostopchina 1996). The consequences of assuming the circumstellar matter to reside in optically thick clumps have been analyzed by Mitskevich (1995a,b). While certainly not all Herbig Ae/Be stars display deep minima, the difference may be merely one of inclination, and the concept of a clumpy circumstellar environment is likely to be relevant for all Herbig Ae/Be stars.

Magnetic models

It has been suggested that Herbig Ae/Be stars may have magnetic fields at their surfaces which are strong enough to force a stellar wind to co-rotate up to the Alfvénic radius. Lines formed inside this radius would exhibit a double-peaked profile, while lines formed inside plus outside the Alfvénic radius would display a P Cygni profile. Such a model has been used to explain the Hα profiles seen in AB Aur (Beskrovnaya et al. 1991).

If the magnetic fields have much structure, then line profiles may be modulated with the period of

[1] Recently the group has also been called UXors, after UX Orionis, thus reminiscent of FUors and EXors (Herbst et al. 1994). However, while FUors and EXors are almost certainly related accretion driven phenomena, the UX Ori type stars represent a completely different type of physical process, and we therefore believe UXor is a misnomer.

rotation, with smaller periods originating closer to the star (Praderie et al. 1986; Catala et al. 1986).

Winds with velocity gradients

In a study of classical Be stars, which can be readily applied to Herbig Ae/Be stars, Cidale & Ringuelet (1993) showed that different velocity gradients at the onset of the wind can result in very different Hα profiles, ranging from single-peaked emission to P Cygni profiles to double-peaked emission in order of decreasing velocity gradients.

Rotation

A rotating star/envelope configuration will give rise to characteristic double-peaked emission lines, and if there is also some expansion of the envelope, a large variety of profiles can be achieved (e.g. Conti & Leep 1974).

7. Analysis and discussion

7.1. *Types of profiles*

Even a cursory examination of the atlas of Hα emission line profiles in Fig. 1 reveals an almost bewildering amount of structure. In this section we discuss the classification system that we have devised to analyze Hα emission line profiles.

The purpose of a classification system is to produce some order into a large and complex data set, by grouping together similar but not precisely identical objects, and classification is therefore done at the expense of detail. A data set can often be classified in a variety of ways; a successful classification system must, firstly, to some extent be simple to use, and, secondly, be meaningful, in the sense that the classification must reflect something of an underlying physical process.

We have considered three existing classification systems of line profiles, namely those of Beals (1951), Ulrich & Knapp (1979) and Finkenzeller & Mundt (1984). The Beals classification considers eight groups of line profiles found in P Cygni type stars, but includes classes with broad absorption lines not seen in our spectra, and moreover not all of our observed profiles are easily fit into this description. The Ulrich & Knapp classification is an empirical system derived from inspection of a large number of Hα profiles of young stars, it contains six classes and most of our profiles could fit into this system. It does, however, lack an underlying idea, and is therefore not as useful as it could have been. Finkenzeller & Mundt considered Herbig Ae/Be stars, and used a system of three classes, which accounted for most of their stars. It is, however, too simple to describe the varieties of profiles we see. Consequently, in the following we outline a classification scheme which we believe is useful for the study of Hα profiles in young stars.

The profiles in Fig. 1 can all be understood if we assume that they are the result of an interplay between an underlying symmetrical emission line and one or more superposed absorbers. What gives a profile its characteristic shape is then defined by 1) the width of the emission, 2) the characteristic velocity of the absorbing material, and 3) the strength (depth and width) of the absorption. The best *single* parameter to characterize this interplay between emission and absorption is the relative height of a secondary peak to the primary peak. Since additionally the absorption can sit both on the blue as well as on the red side of the emission peak, this parameter must be included. We here use the following two-dimensional classification system, with four classes depending on the secondary-to-primary peak ratio, and two branches, corresponding to blue or redshifted absorptions. The types are illustrated schematically in Fig. 4.

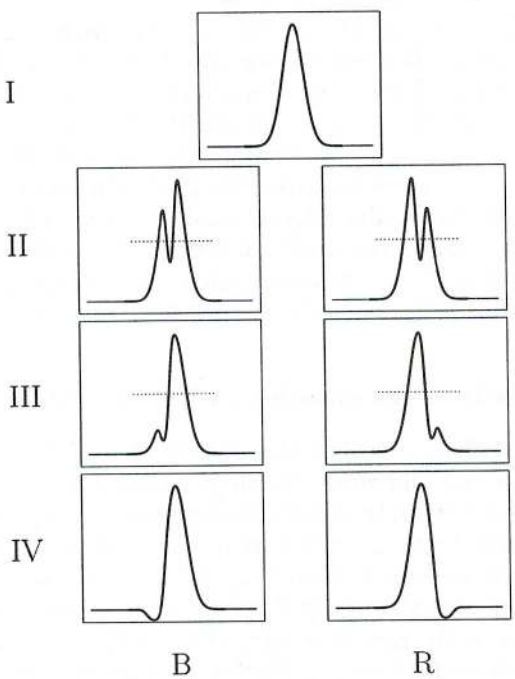

Fig. 4. A classification scheme for Hα emission line profiles. The dotted line indicates 50% of maximum line intensity

- *Type I* profiles are symmetric with no or only very slight influence from absorption features.
- *Type II* profiles have two peaks, and the secondary peak exceeds half the strength of the primary peak. In cases with very weak absorption the double-peaked profile may degenerate to a single peak with a hump.
- *Type III* profiles have two peaks, and the secondary peak is less than half the strength of the primary peak.
- *Type IV* profiles are P Cygni or inverse P Cygni profiles, that is, the absorption has a sufficient velocity to be present beyond the wing of the underlying emission line, and no secondary peak is visible.

Depending on whether the secondary peak is located bluewards or redwards of the primary peak, a second

parameter B or R is appended to the roman numeral. Among the type IV profiles, normal P Cygni profiles are labelled B and inverse P Cygni profiles are labelled R.

In a significant number of cases, more than one absorption is present, and such multiple absorptions are indicated by the suffix 'm'. In rare cases, this could lead to two different classifications, e.g. CU Cha can equally well be classified IV-Bm and II-Rm (we have chosen the former, considering the P Cygni profile the physically more important feature).

7.2. *The profiles of T Tauri stars vs Herbig Ae/Be stars*

In Fig. 5 we show a histogram of the Hα profile classes divided between T Tauri stars and Herbig Ae/Be stars; the two FUors are not included. With 43 T Tauri stars the statistics is reasonably good, while with only 18 Herbig Ae/Be stars the statistical significance is less good. Nonetheless, it is clear that the two categories of stars have certain differences in their Hα profiles.

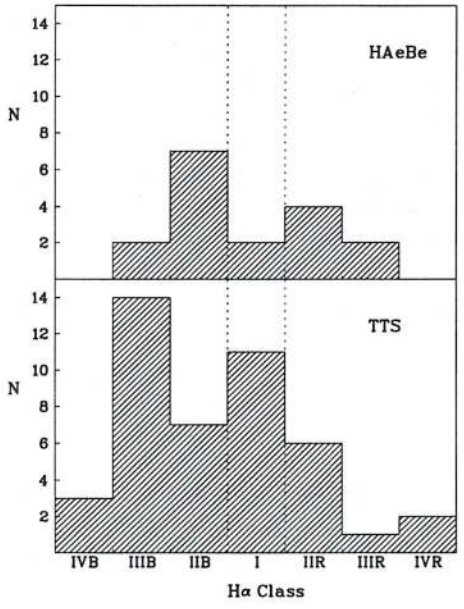

Fig. 5. A histogram of Hα profile classes for 43 T Tauri stars and 18 Herbig Ae/Be stars. The two FUors FU Ori and Z CMa are not included

Among the T Tauri stars, 25% of all our stars have symmetric profiles, indeed such profiles are the second-most common profile type. For Herbig Ae/Be stars, on the other hand, only 11% (2 out of 18 stars) have symmetric profiles. By far the most common profile type for Herbig Ae/Be stars is type II, with doublepeaked lines having deep central absorptions. The most common profile type among T Tauri stars is type IIIB, which 33% (14 out of 43) stars display.

P Cygni and inverse P Cygni profiles (type IV) are few among the T Tauri stars, and only one case is seen in our sample of Herbig Ae/Be stars.

The distribution of blue and redshifted absorptions is slightly higher for blue absorptions than red among the Herbig Ae/Be stars (10 vs. 6), whereas there is a significantly larger number of blueshifted relative to redshifted absorptions (24 vs. 9) among the T Tauri stars.

These results are further discussed in Sect. 7.6.

7.3. *Line widths and high velocity wings of Hα*

Almost all the Hα profiles in Fig. 1 show extensive wings reaching velocities of several hundred km/s. As an example we show in Fig. 6 the base of a very high signal-to-noise spectrum of RU Lup, with evidence of symmetric wings extending to beyond ±900 km/s. Our general spectra have much less S/N, and such extremely high velocity wings, if present, could not be measured in all of our atlas spectra. Moreover, the normalization of our spectra could, at least in principle, introduce subtle changes in the extended wings because of the limited spectral range over which the echelle order permits to define a continuum. We have therefore, upon careful examination of our spectra, chosen to measure the line width at 1/40th of the maximum line intensity. Dotted horizontal lines in each of the spectra of Fig. 1 show the $I_{\max}/40$ level. This is a conservative measure which allows a meaningful determination of the line width even for our lowest S/N spectra, and which would not be affected by putative normalization problems. However, as is abundantly clear from Fig. 6, even the $I_{\max}/40$ level will dramatically underestimate the true line-width in the cases when very faint and extremely high velocity wings are present. In most cases we believe the $I_{\max}/40$ width will give a valid, albeit conservative estimate of the extent of the line wings, and it is certainly useful for analyzing the asymmetries of the line wings. An additional problem is that for lines with low-velocity absorption, which makes a central absorption that cuts out the true peak of the emission line, the $I_{\max}/40$ level is lower than it would otherwise have been. These limitations should be kept in mind in the following discussion.

In Table 1 Col. 9 we list the $I_{\max}/40$ velocities for the blue and red wings of all stars. While we obviously would expect all type IV stars to show asymmetries, we additionally find that many other stars have significant differences between their blue and red wings, possibly indicating the presence of very high velocity absorption. In Fig. 7 we have plotted the blue and red $I_{\max}/40$ velocities against each other, where T Tauri stars are marked with a +, Herbig AeBe stars with a □ and FU Orionis stars with a ×. The three diagonal dotted lines indicate the expected location for stars which have symmetric wings within ±15 km/s. Stars with significant blue absorption fall below this line (note especially the positions of the two FUors and the

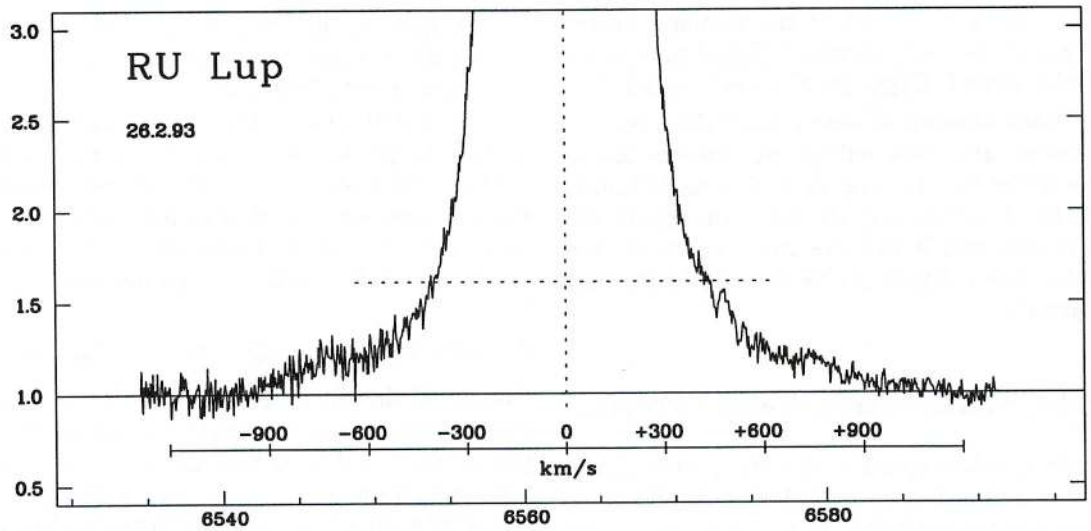

Fig. 6. The wings of RU Lup seen in a very high signal-to-noise spectrum. The spectrum of RU Lup shown in Fig. 1 was taken on another night. The horizontal dotted line represents the $I_{max}/40$ line, similar to the ones shown in Fig. 1

FUor like T Tauri star CO Ori), and stars with strong red absorption move to the left of the line. We have no reliable way of estimating how many stars suffer simultaneous blue and red absorption, and ignore this possibility in the following.

In Fig. 8 we show a histogram of the number of stars in 30 km/sec bins of the parameter ΔV_{wing}, which is the sum of the blue and red wing velocities listed in Table 1. The central bin of ±15 km/s corresponds to the diagonal lines in Fig. 7. We see that 18 out of 63 (35%) of our stars have wings that are symmetric. This is larger than the number of type I stars in Fig. 5, because also stars with central absorptions can have symmetric wings. When from our sample of 63 stars we subtract the 18 stars with symmetric wings and the 5 T Tauri stars of type IV (P Cygni and inverse P Cygni profiles) and the 2 FUors, we are left with the surprising result that 38 stars have asymmetric wings. As can be seen from Fig. 7, 11 of these stars are Herbig Ae/Be stars, and the remaining 27 are T Tauri stars, that is, roughly two thirds of both groups of stars have asymmetric line wings. This curious result is further discussed in Sect. 7.6.

The actual velocities measured at $I_{max}/40$ are plotted in Fig. 9, which shows that typical wing velocities are in the range 250 to 400 km/s, with essentially no difference in the range of blue and red velocities. As can be seen in Fig. 7, Herbig Ae/Be stars tend to have somewhat larger wing-velocities than T Tauri stars.

7.4. *Equivalent widths*

In Fig. 10 we show a histogram of equivalent widths for all stars in the atlas. The measurements refer only to the emission part of the line, and possible absorption beneath the continuum is disregarded. We should from the beginning warn that this distribution is likely to be seriously affected by selection effects. Our stars were chosen because we *knew* that they had Hα in emission, so young stars with weak Hα emission which might have been overlooked in Hα emission surveys are underrepresented in this work. Also, as we discuss in Paper II, the equivalent width of Hα can change considerably for a given star. Keeping these limitations in mind, the snapshot of Hα emission of our sample of stars shows that although most of the stars observed have equivalent widths exceeding 10 Å the bin in Fig. 10 with the weakest emission (<10 Å) is clearly the most populated, and also that there is a steady decrease in the numbers of stars with increasing Hα emission equivalent width. The star with highest equivalent width is the T Tauri star HO Lup, which with an equivalent width of 239 Å is close to two orders of magnitude larger than the weakest emission line stars. Each column in Fig. 10 is divided between T Tauri stars and Herbig Ae/Be stars, and we see that, to within the statistical noise in the data, the two categories of stars have the same equivalent widths, and show the same decrease in numbers with increasing equivalent width. Of course, since A and B stars have much brighter continua than K and M stars, it follows that the *strength* of the emission of Herbig stars is much higher than for T Tauri stars.

We have tried to quantify the line asymmetries caused by the absorptions commonly influencing the line profile by measuring the equivalent width longwards and shortwards of the rest wavelengths listed in Table 1. We plot these red and blue equivalent widths against one another in Fig. 11. Perfectly symmetric emission lines lie on the 45° dotted line, and emission lines with the same fraction of asymmetry will be lying on lines passing through

the origin but with other angles. From the distribution of classifications in Fig. 5 we know that for the T Tauri stars, asymmetric lines with blue absorptions are significantly more common than similar ones with red absorption. Figure 11 shows additionally that emission lines with small equivalent widths have comparable percentages of blue and red absorption. However, among the relatively few stars with total equivalent widths of 70 Å or so, stars with blue absorptions are not only more common, but their asymmetries are also more pronounced.

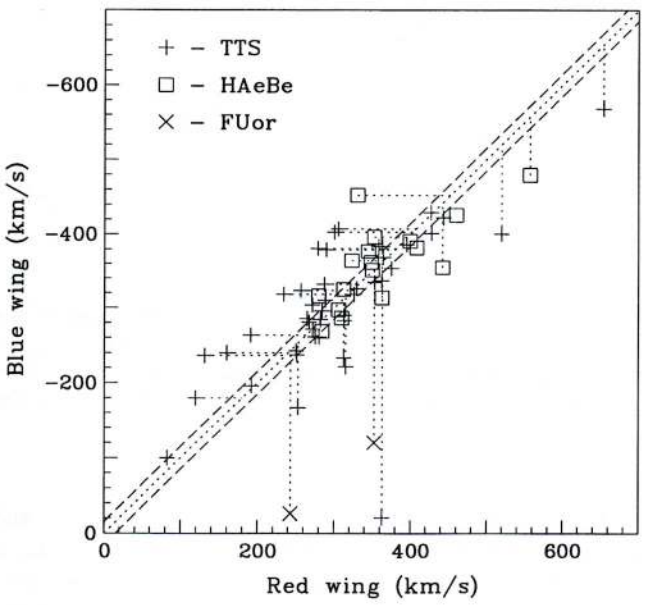

Fig. 7. Velocities of the red wing versus the blue wing at $I_{max}/40$ for all stars in the atlas

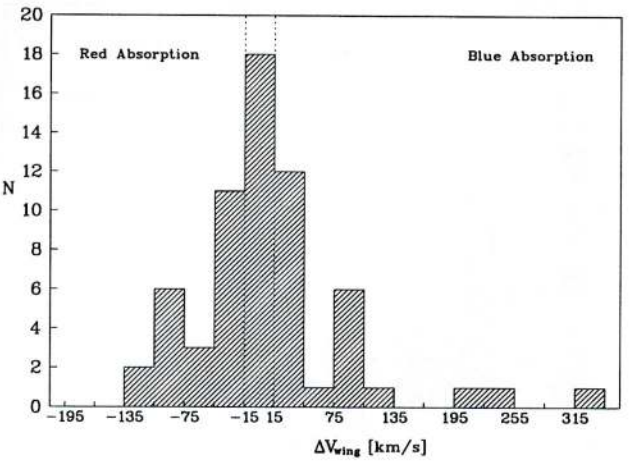

Fig. 8. A histogram of the sum of the blue and red wing velocities showing the number of stars in 30 km/s bins. Stars with large red absorptions have small red wing velocities and therefore the sum of the wing velocities become negative, and vice versa for the stars with large blue absorptions

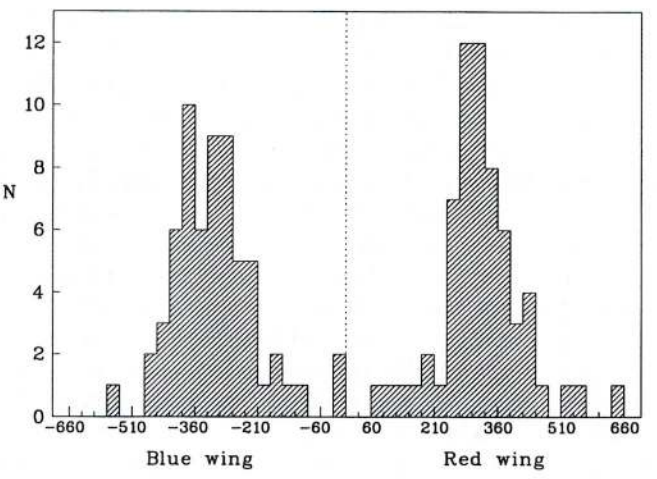

Fig. 9. A histogram of the blue and red wing velocities $I_{max}/40$ in 30 km/s bins for all stars in the atlas

7.5. *The absorption dips*

We are discussing the strength, kinematics and nature of the absorption dips in more detail in Paper II, and here only present some basic statistical facts about these features.

Absorption is evident in at least 50 out of our 63 stars, which is the number of stars of types II-III-IV. Even the type I sources can have subtle asymmetries, as for example seen in the spectrum of Sz 77. The strength of this absorption has a very large range, from manifesting itself merely as a depression in the line profile (e.g. AS 206), to reaching well beneath the continuum (e.g. AK Sco). Strong absorption is common, in 17 out of 63 stars the absorption goes beneath the continuum level, and there is no statistically significant difference between it happening in T Tauri stars (10 out of 43) or in Herbig Ae/Be stars (5 out of 18).

Absorption dips can be narrow (e.g. CU Cha) as well as broad (e.g. Haro 1-16), suggesting that the absorbing material may span a range of velocities. In some cases the absorption features split into several dips (e.g. AS 205) or several absorption features are seen, for example on either side of the emission peak, as seen in HT Lup. Such stars have an '*m*' in their classification, and 23 of our 63 stars are marked this way. Multiple absorptions are thus a frequent feature.

7.6. *Profiles versus models*

We have in this paper presented a statistical analysis of a large collection of high resolution Hα line profiles of young stars. Variability of these lines, to be discussed in Paper II, provides further important constraints on the mechanisms which produce the observed line profiles, and we therefore

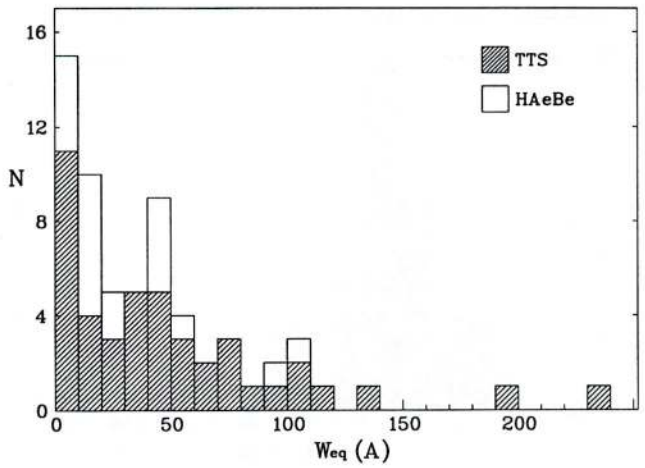

Fig. 10. A histogram of the equivalent widths for all stars in the atlas. For each column it is indicated how many stars are T Tauri stars and Herbig Ae/be stars. The measured equivalent widths refer only to the emission part of the line

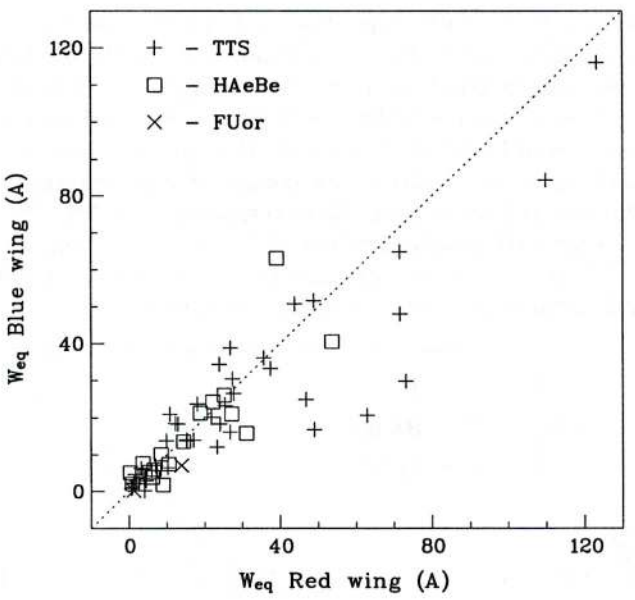

Fig. 11. The equivalent width of the part of the emission line bluewards of the stellar rest velocity plotted against the equivalent width of the similar red emission component for all stars in the atlas. The dotted lines help to visualize the symmetries and asymmetries in the distribution

defer a more detailed comparison with models to Paper II. However, a few remarks will already be made here.

In Sect. 7.3 we found that approximately two thirds of both T Tauri stars and Herbig Ae/Be stars show asymmetries of their extended line wings at the $I_{max}/40$ level. This could be due to three different mechanisms. Firstly, it may be caused by high velocity absorbing material. Given that there is ample evidence for the presence of absorbing material at lower velocities in our spectra, it cannot be excluded that some exists also at higher velocities. Secondly, the emitting region in which the Hα line is formed may not be spherically symmetric, but could for example be spiralshaped, as expected in the magnetohydrodynamic models which have appeared in recent years (e.g. Königl 1991; Hartmann et al. 1994). If so, the blue/red wing asymmetries should change with the orbital period of the star. Finally, even if the line forming regions should be spherically symmetric, it is conceivable that the small amount of very high velocity material is optically thin and clumpy, and that the high velocity line asymmetries are caused by emission from such clumps. At the moment it is impossible to give preference to any of the above models on the basis only of the present data, but it appears that further study of high velocity wings of both T Tauri stars and Herbig Ae/Be stars could provide valuable constraints on emission line models.

The types of profiles of T Tauri stars differ from those of Herbig Ae/Be stars, as discussed in Sect. 7.2 and shown in Fig. 5, suggesting that different line formation mechanisms may be at play. The very small number of symmetric lines and the ubiquity of deep central absorptions for Herbig Ae/Be stars is consistent with a single mechanism as the principal shaper of the profiles of these stars, with only minor contributions from other phenomena. The clumpy interstellar environment model elaborated by Grinin and collaborators (see Sect. 6) is a very attractive hypothesis because it can explain not only almost all the Hα profiles we observe, but also a large number of other types of observations. The fact that the large majority of our Herbig Ae/Be stars show deep central absorptions suggests that the equatorial torus of obscuring material must be very thick, unless our sample of stars are mostly having the equatorial plane close to the line of sight, which is highly unlikely.

The situation is more complex for the T Tauri stars, and it is very doubtful that a single model can account for the rich variety of profiles we see. The clumpy circumstellar environment model is at least applicable to some T Tauri stars (e.g. Grinin & Mitskevich 1991; Mitskevich 1995a,b), foremost among them RY Lup, which in terms of its line profile, its photometric variability and color changes, and polarimetric variations closely mimics the behaviour of Herbig Ae/Be stars with deep minima, despite being a K star (e.g Gahm et al. 1989, 1993; Drissen et al. 1989). However, other models discussed in Sect. 5 can claim equal success in explaining line profiles for specific stars. Below we discuss various aspects of different models of line formation in T Tauri stars, as applied to our atlas of line profiles.

Spherical symmetric models of winds driven by Alfvén waves (i.e. Hartmann 1982), seem adequate to produce the type IV-B profiles, but these correspond to only 7% of the cases in our sample.

The type III-B profiles seem reasonably well represented by the stochastic wind model of Grinin & Mistkevich (1991), although it fails to adequately account for the separation between the two emission peaks (far too narrow), resulting in the blue absorptions to be located at much lower velocities than in our profiles. Another difficulty is the presence of a secondary blue absorption at higher velocities. In subsequent work (Mitskevitch et al. 1993), the models and observations disagree in the excessive sharpness of the transition between the main emission peak and the blue absorption, while on the contrary the red wing of the secondary emission peak is systematically less abrupt than shown in the great majority of our spectra. However this model looks quite adequate to the Hα profile observed for the star AS 353A but for the more extended red wing present in the data.

This same star and in general type III-B profiles where the absorption goes below the continuum, could broadly speaking also be partially accommodated by a decelerating wind model such as Kuan & Kuhi (1975), even if it fails to predict for Hα a substantial amount of emission further to the blue of the absorption and a primary emission peaked not centered at the star's rest velocity.

Also a III-B type profile with narrower absorption centered near the rest velocity of the star, much like the one of EZ Ori, is also reproduced by the model proposed for SU Aur by Johns & Basri (1995).

The series of models proposed by Calvet & Hartmann (1992), where the infall material flows inside two coaxial cones, lead to profiles of type II-R or III-R, depending on the adopted parameters. From the 6 stars in our sample belonging to these classes, only GQ Lup shows an Hα line that can be reasonably well described by these models, if quite restrictive conditions are adopted.

Broadly speaking, all models in the literature adopt a photosphere with temperatures around 4500 K and a line forming region not exceeding 10 stellar radii with an electron temperature between 5000 K and 10000 K, although in some models (Hartmann et al. 1982) the temperature tends to peak at $\sim 3R_*$ where it reaches the higher values needed for the balance of the cooling and heating rates. For the wind models the mass loss rate is between 10^{-9} to 10^{-8} $M_\odot$/yr and the maximum velocity for the wind around 300 km/s, or lower in those models invoking high turbulence. In the infall models the maximum velocity is of the same order and the accretion ranges from 10^{-7} to 10^{-8} $M_\odot$/yr. This results in the presence of high density regions, and the need to invoke lower gas temperatures, around 7000 K (Calvet & Hartmann 1992).

Altogether, while there is reasonable agreement on the range of adopted values for the mass loss, the mechanism for producing the observed Hα lines, as well as the dynamics and geometry of the lineforming region is still uncertain. In any case, if these matters are to be clarified and the Hα line profile kept as a useful probe, it is quite clear that an adequate treatment of the H atom levels population and of radiative transfer are unavoidable.

Equally important is the simultaneous study of other lines that will provide further constraints on the physical and dynamic conditions prevailing in the outer layers and immediate surroundings of pre-main sequence stars.

Acknowledgements. We thank Elena Ortiz and Vladimir Grinin for sending preprints prior to publication.

References

Andersen J., Lindgren H., Hazen M.L., Mayor M., 1989, A&A 219, 142
Appenzeller I., Wolf B., 1977, A&A 54, 713
Appenzeller I., Wagner S., 1989, A&A 225, 432
Appenzeller I., Mundt R., Wolf B., 1978, A&A 63, 289
Appenzeller I., Jankovics I., Jetter R., 1986, A&AS 64, 65
Baade D., Stahl O., 1989, A&A 209, 255
Batalha C.C., Basri G., 1993, ApJ 412, 363
Bateson F.M., McIntosh R., Brunt D., 1990, Publ. of Var. Star Section of the Roy. Astron. Soc. of New Zealand No. 16, 49
Beals C.S., 1951, Pub. Dominion Obs. 9, 1
Bertout C., Carrasco L., Mundt R., Wolf B., 1982, A&AS 47, 419
Beskrovnaya N.G., Pogodin M.A., Tavasov A.E., Sherbakov A.G., 1991, Soviet Ast. Lett. 17, 349
Bibo E.A., Thé P.S., 1990, A&A 236, 155
Bibo E.A., Thé P.S., 1991, A&AS 89, 319
Bibo E.A., Thé P.S., Dawanas D.N., 1992, A&A 260, 293
Bouvier J., Appenzeller I., 1992, A&AS 92, 481
Böhm K.-H., Raga A.C., 1987, PASP 99, 265
Böhm K.-H., Solf J., 1994, ApJ 430, 277
Böhm T., Catala C., 1994, A&A 290, 167
Brandner W., Bouvier J., Grebel E.K., Tessier E., de Winter D., Beuzit J.-L., 1995, A&A 298, 818
Byrne P.B., 1986, Irish Astron. J. 17, 294
Calvet N., Hartmann L., 1992, ApJ 386, 239
Calvet N., Basri G., Kuhi, 1984, ApJ 277, 725
Calvet N., Hartmann L., Hewett R., 1992, ApJ 386, 229
Catala C., 1989, in Low Mass Star Formation and Pre-Main Sequence Objects, ESO Workshop, Reipurth B. (ed.), p. 471
Catala C., 1994, in The Nature and Evolutionary Status of Herbig Ae/Be Stars, ASP Conf. Ser. 62, Thé P.S., Perez M.R., van den Heuvel E.P.J. (eds.), p. 91
Catala C., Felenbok P., Czarny J., Talavera A., Boesgaard A.M., 1986, ApJ 308, 791
Chavarria-K. C., de Lara E., Finkenzeller U., Mendoza E.E., Ocegueda J., 1988, A&A 197, 151
Cidale L.S., Ringuelet A.E., 1993, ApJ 411, 874
Cohen M., Kuhi L.V., 1979, ApJS 41, 743
Conti P.S., Leep E.M., 1974, ApJ 193, 113
Corcoran D., Ray T.P., 1995, A&A 301, 729
Covino E., Terranegra L., Vittone A.A., Russo G., 1984, AJ 89, 1868
DeCampli, 1981, ApJ 244, 124
de la Reza R., Quast G., Torres C.A.O., Mayor M., Meylan G., Llorente de Andres F., 1986, in New Insights in Astrophysics, ESA SP-263, p. 107

de la Reza R., Torres C.A.O., Quast G., Castilho B.V., Vieira G.L., 1989, ApJ 343, L61
Devaney M.N., Thiebaut E., Foy R., Blazit A., Bonneau D., Bouvier J., de Batz B., Thom Ch., 1995, A&A 300, 181
Drissen L., Bastien P., St-Louis N., 1989, AJ 97, 814
Dutrey A., Guilloteau S., Simon M., 1994, A&A 286, 149
Edwards S., 1979, PASP 91, 329
Edwards S., Hartigan P., Ghandour L., Andrulis C., 1994, AJ 108, 1056
Eislöffel J., Solf J., Böhm K.H., 1990, A&A 237, 369
Elias J.H., 1978, ApJ 224, 453
Evans, Levreault, Beckwith S., Skrutskie, 1987, ApJ 320, 364
Evans A. Davies J.K., Kilkenny D., Bode M.F., 1989, MNRAS 215, 537
Fernández M., Ortiz E., Eiroa C., Miranda L.F., 1995, A&AS 114, 439
Finkenzeller U., Mundt R., 1984, A&AS 55, 109
Finkenzeller U., Basri G., 1987, ApJ 318, 823
Franchini M., Castelli F., Stalio R., 1991, A&A 242, 449
Franchini M., Covino E., Stalio R., Terranegra L., Chavarria-K.C., 1992, A&A 256, 525
Friedemann C., Reimann H.G., Gurtler J., Toth V., 1993, A&A 277, 184
Gahm G.F., Fischerström C., Liseau R., Lindroos K.P., 1989, A&A 211, 115
Gahm G.F., Liseau R., Gullbring E., Hartstein D., 1993, A&A 279, 477
Gameiro F., Lago M.T.V.T., 1995, Proc. IAU Symp. 176. In: Strassmeier K.G. (ed.), p. 170
Garrison L.M., Anderson C.M., 1977, ApJ 218, 438
Gauvin L.S., Strom K.M., 1992, ApJ 385, 217
Giovannelli F., Errico L., Vittone A.A., Rossi C., 1991, A&AS 87, 89
Giovanelli F., et al., 1995, A&AS 114, 341
Goodrich R.W., 1993, ApJS 86, 499
Graham J.A., 1992, PASP 104, 479
Graham J.A., 1993, PASP 105, 561
Graham J.A., Phillips A.C., 1987, PASP 99, 91
Grinin V.P., 1992, A&A Trans. 3, 17
Grinin V.P., Mitskevich A.S. 1991, Ap&SS 185, 107
Grinin V.P., Tambovtseva L.V., 1995, A&A 293, 396
Grinin V.P., Rostopchina A.N., 1996, Russian Astron. J., (in press)
Grinin V.P., Thé P.S., de Winter D., et al., 1994, A&A 292, 165
Hamann F., 1994, ApJS 93, 485
Hamann F., Persson S.E., 1992, ApJS 82, 285
Hartigan P., et al., 1991, ApJ 382, 617
Hartmann L., 1982, ApJS 48, 109
Hartmann L., Edwards S., Avrett, 1982, ApJ 261, 279
Hartmann L., Kenyon S.J., 1990, ApJ 261, 279
Hartmann L., Calvet N., 1995, AJ 109, 1846
Hartmann L., Kenyon S.J., Hewett R., Edwards S., Strom K.M., Strom S.E., Stauffer J.R., 1989, ApJ 338, 1001
Hartmann L., Hewett R., Calvet N., 1994, ApJ 426, 669
Herbig G.H., 1960, ApJS 4, 337
Herbig G.H., 1962, Advances Astron. Astrophys. 1, 47
Herbig G.H., 1966, Vistas Astron. 8, 109
Herbig G.H., 1968, ApJ 152, 439
Herbig G.H., 1977, ApJ 217, 693
Herbig G.H., 1989, in ESO workshop on Low Mass Star Formation and Pre-Main Sequence Objects, Reipurth Bo (ed.), p. 447
Herbig G.H., 1994, in The Nature and Evolutionary Status of Herbig Ae/Be Stars, ASP Conf. Ser. 62, Thé P.S., Perez M.R., van den Heuvel E.P.J. (eds.), p. 3
Herbig G.H., Jones B., 1983, AJ 88, 1040
Herbig G.H., Bell K.R., 1988, Third Catalog of Emission-Line Stars of the Orion Population, Lick Observatory Bulletin No. 1111
Herbst W., Holtzman J.A., Klasky R.S., 1983, AJ 88, 1648
Herbst W., Herbst D.K., Grossman E.J., Weinstein D., 1994, AJ 108, 1906
Hessman F.V., Eislöffel J., Mundt R., Hartmann L.W., Herbst W., Krautter J., 1991, ApJ 370, 384
Heyer M.H., Graham J.A., 1989, PASP 101, 816
Hoffmeister C., 1949, Astron. Nachr. 278, 24
Hughes J., Hartigan P., Krautter J., Kelemen J., 1994, AJ 108, 1071
Hutchinson M.G., Evans A., Davies J.K., Bode M.F., 1989, MNRAS 237, 683
Innes R.T.A., 1927, Southern Double Star Catalogue, Union Observatory, Johannesburg, South Africa
Johns C.M., Basri G., 1995, ApJ 449, 341
Joy A.H., 1945, ApJ 102, 168
Kawabe R., Ishiguro M., Omodaka T., Kitamura Y., Miyama S.M., 1993, ApJ 404, L63
King J., 1993, AJ 105, 1087
Kolotilov E.A., 1977, Astrophys. 13, 17
Königl A., 1991, ApJ 370, L39
Koresko C.D., Beckwith V.W., Ghez A.M., Matthews K., Neugebauer G., 1991, AJ 102, 2073
Krautter J., Appenzeller I., Jankovics I., 1990, A&A 236, 416
Kuan P., Kuhi L.V., 1975, ApJ 199, 148
Lago M.T.V.T., 1979, Ph.D Thesis, Univ. Sussex
Lago M.T.V.T., 1982, MNRAS 198, 445
Lehmann T., Reipurth B., Brandner W., 1995, A&A 300, L9
Leinert C., Haas M., Richichi A., Zinnecker H., Mundt R., 1991, A&A 250, 407
Leinert Ch., Richichi A., Weitzel N., Haas M., 1994, in Nature and Evolutionary Status of Herbig Ae/Be Stars, Thé P.S., Pérez M.R., van den Heuvel E.P.J. (eds.), p. 155
Levreault R.M., 1988, ApJS 67, 283
Levreault R.M., 1988, ApJ 330, 897
Lightfoot J.F., 1989, MNRAS 239, 665
Lindgren H., Gilliotte A., 1989, ESO Operating Manual No. 8
Liseau R., Lindroos K.P., Fischerström C., 1987, A&A 183, 274
Magazzú A., Martin E.L., Rebolo R., 1991, A&A 249, 149
Maihara T., Kataza H., 1991, A&A 249, 392
Mathieu R.D., Adams F.C., Latham D.W., 1991, AJ 101, 2184
Mathieu R.D., Adams F.C., Fuller G.A., Jensen E.L.N., Koerner D.W., Sargent A.I., 1995, AJ 109, 2655
Mitskevich A.S., 1995a, A&A 298, 219
Mitskevich A.S., 1995b, A&A 298, 231
Mitskevich A.S., Natta A., Grinin V.P., 1993, ApJ 404, 751
Moore C.E., A Multiplet Table of Astrophysical Interest, 1972
Moore C.E., Minnaert M.G.J., Houtgast J.A, 1966, The Solar Spectrum 2935Å – 8770Å. Second revision of Rowland's preliminary table of Solar spectrum wavelengths

Mundt R., 1979, A&A 74, 21
Mundt R., 1984, ApJ 280, 749
Natta A., Giovanardi C., Palla F., 1988, ApJ 332, 921
Pedrosa A., Reipurth B., Lago M.T.V.T., 1997, (in preparation) (Paper II)
Penston M.V., Lago M.T.V.T., 1983, MNRAS 202, 77
Penston M.V., Lago M.T.V.T., 1982, Proc. 3rd IUE Conf. ESA-SP176, 95
Perez M.R., Grady C.A., Thé P.S., 1993, A&A 274, 381
Perez M.R., Webb J.R., Thé P.S., 1992, A&A 257, 209
Pettersson B., Reipurth B., 1994, A&AS 104, 233
Poetzel R., Mundt R., Ray T.P., 1989, A&A 224, L13
Pogodin M.A., 1992, Sov. Ast. Lett. 18, 437
Pogodin M.A., 1994, A&A 282, 141
Praderie F., Simon T., Catala C., Boesgaard A.M., 1986, ApJ 303, 311
Pugach A.F., Kovalchuk G.U., 1986, Astron. Nachr. 307, 13
Reipurth B., 1983, A&A 117, 183
Reipurth B., Graham J.A., 1988, A&A 202, 219
Reipurth B., Zinnecker H., 1993, A&A 278, 81
Rucinski S.M., Krautter J., 1983, A&A 121, 217
Sargent A.I., Beckwith S.V.W., 1987, ApJ 323, 294
Schwartz R.D., 1977, ApJS 35, 161
Schwartz R.D., Heuermann R.W., 1981, AJ 86, 1526
Schwartz R.D., Schultz A.S.B., 1992, AJ 104, 220
Stecklum B., Eckart A., Henning T., Loewe M., 1995, A&A 296, 463
Thé P.S., Felenbok P., Cuypers H., Tjin-A-Djie H.R.E., 1985, A&A 149, 429
Thé P.S., De Winter D., Perez M.R., 1994, A&AS 104, 315
Tjin-A-Djie H.R.E., Remijn L., Thé P.S., 1984, A&A 134, 273
Tjin-A-Djie H.R.E., Thé P.S., Andersen J., Nordström B., Finkenzeller U., Jankovics I., 1989, A&AS 78, 1
Ulrich R.K., Knapp G.R., 1979, ApJ 230, L99
Valenti J.A., Basri G., Johns C.M., 1993, AJ 106, 2024
Voshchinnikov N.V., Grinin V.P., Karjukin V.V., 1995, A&A 294, 547
Walker M.F., 1972, ApJ 175, 89
Welty A.D., Barden S.C., Huenemoerder D.P., Ramsey L.W., 1992a, AJ 103, 1673
Welty A.D., Strom S.E., Edwards S., Kenyon S.J., Hartmann L.W., 1992b, ApJ 397, 260
Wolf B., Appenzeller I., Bertout S., 1977, A&A 58, 163

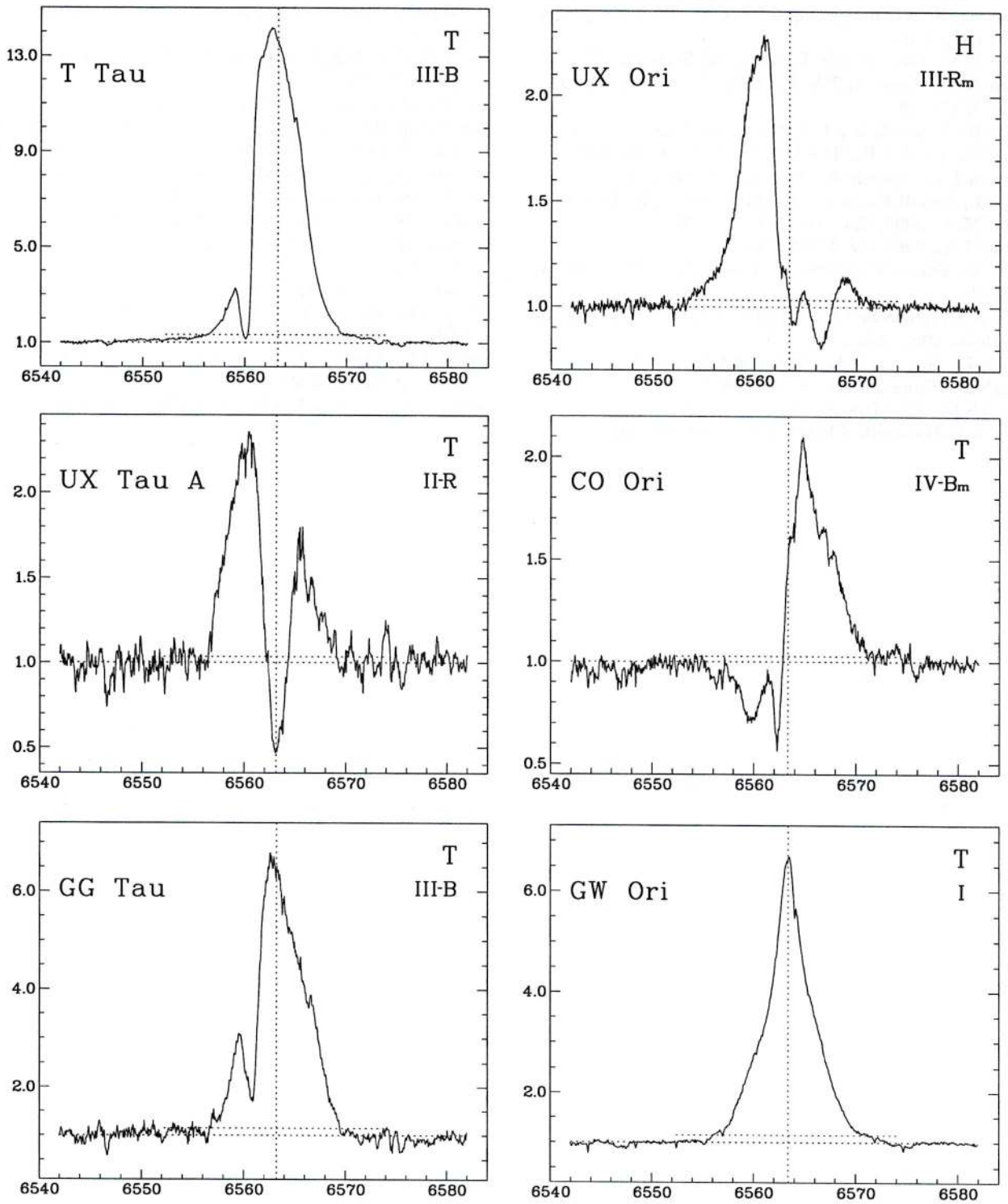

Fig. 1. An atlas of Hα emission line profiles in young stars

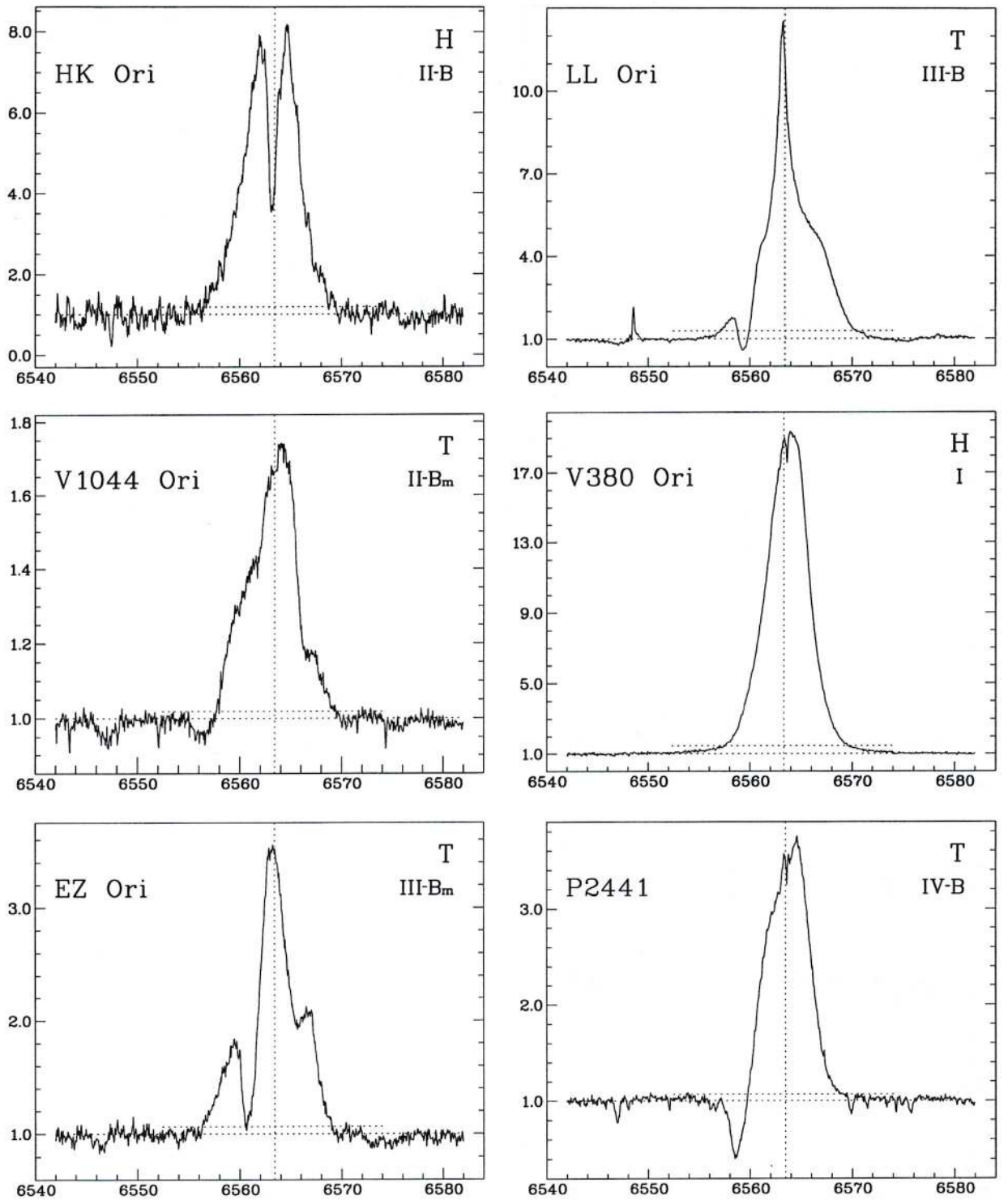

Fig. 1. continued

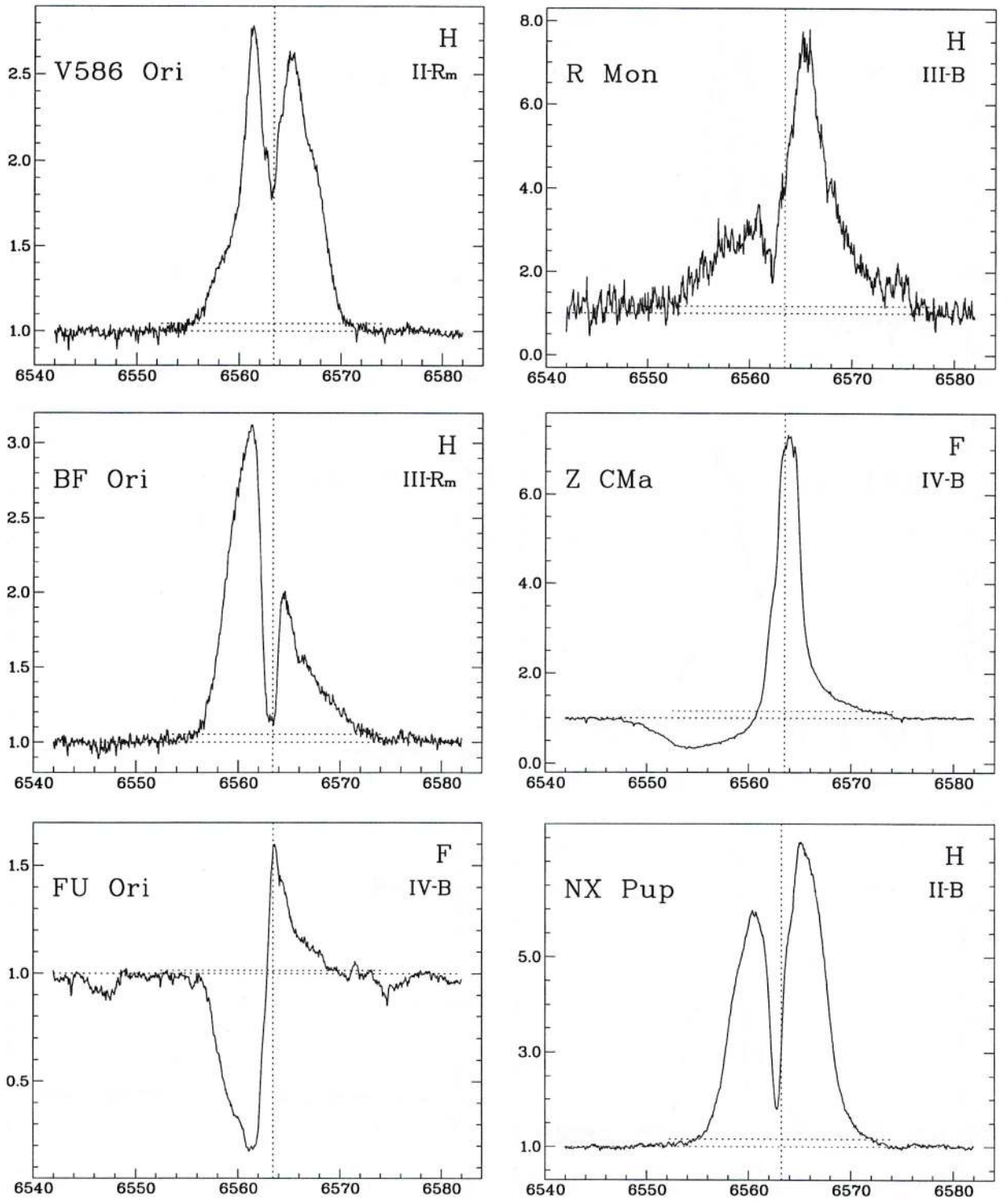

Fig. 1. continued

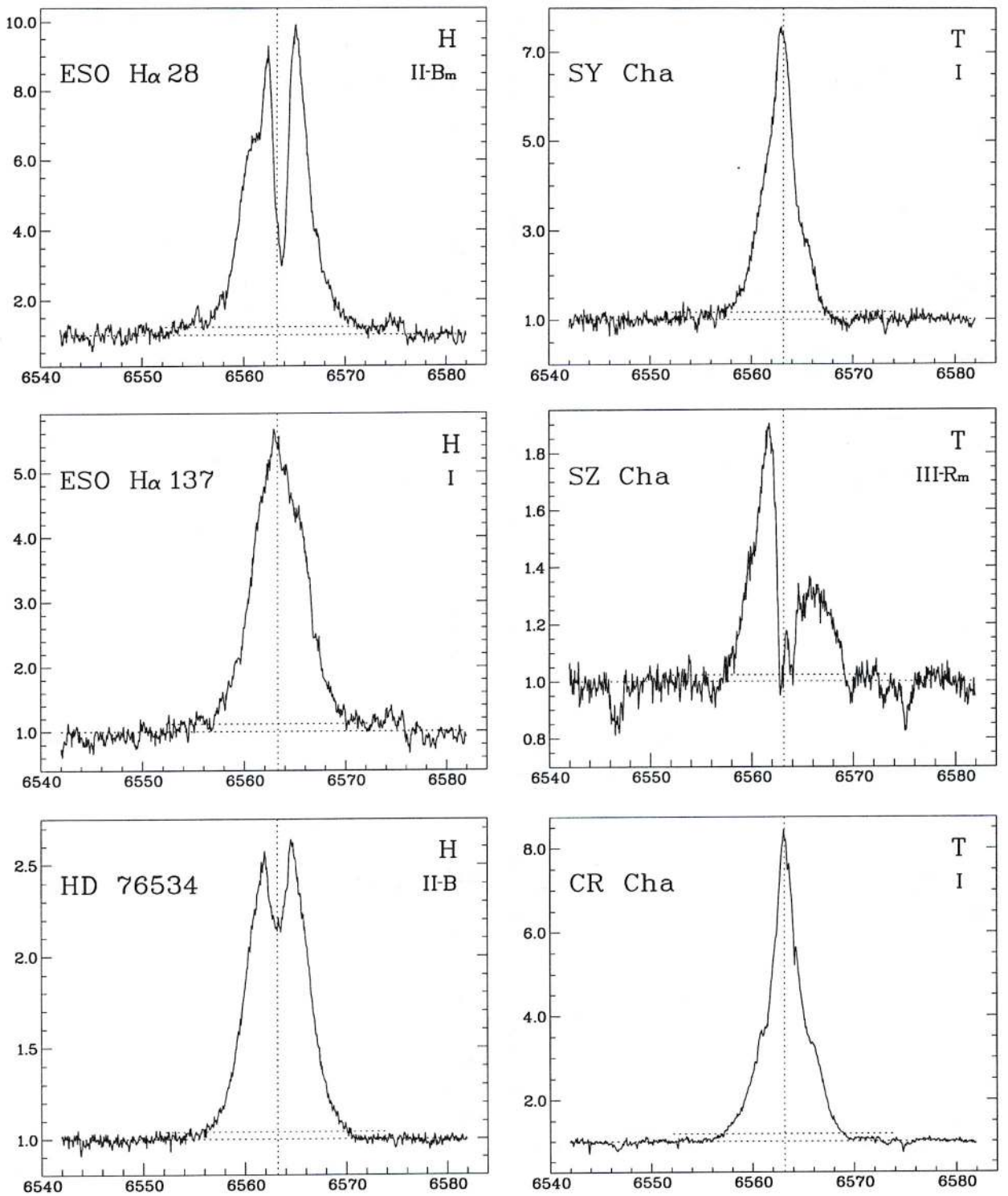

Fig. 1. continued

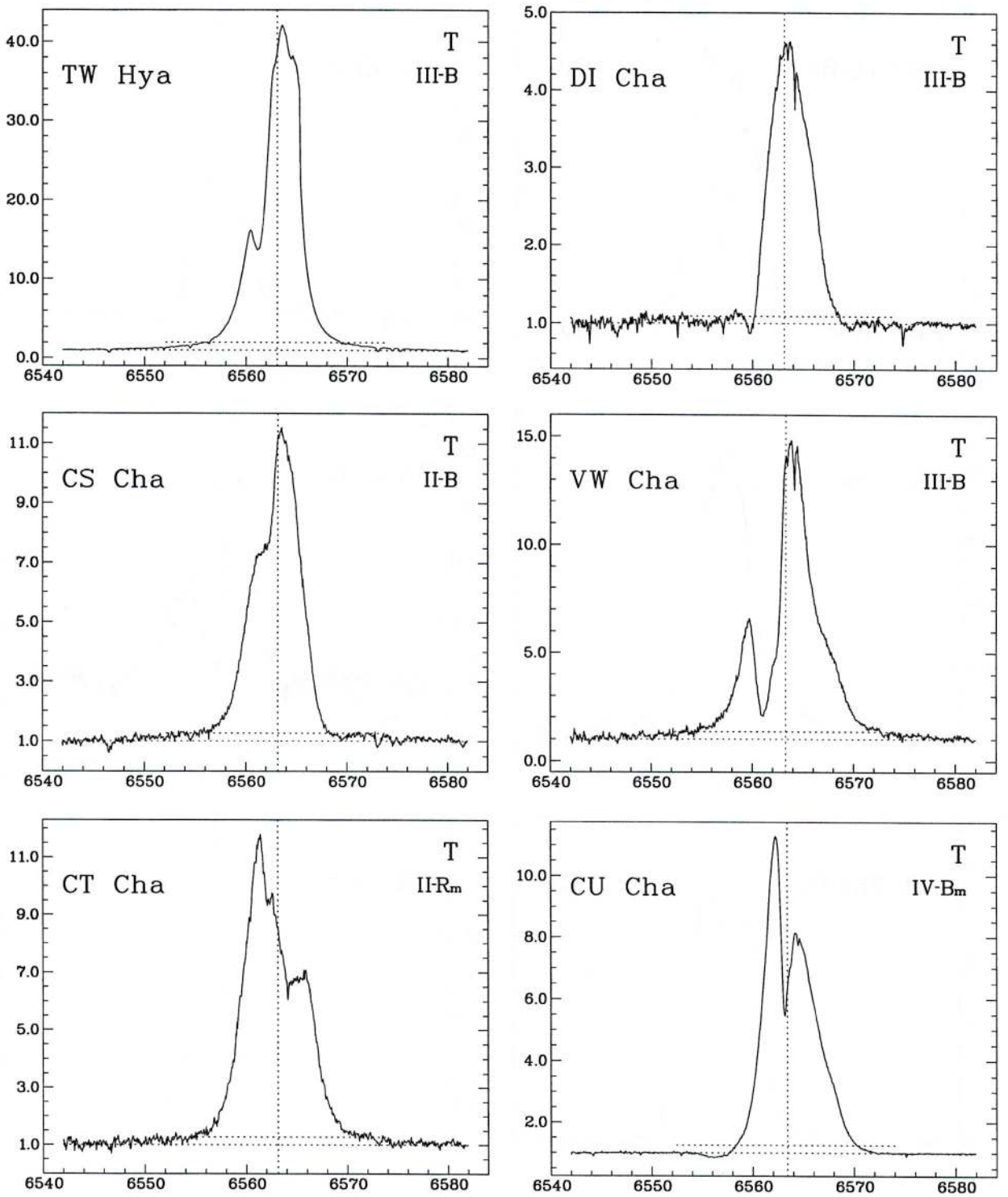

Fig. 1. continued

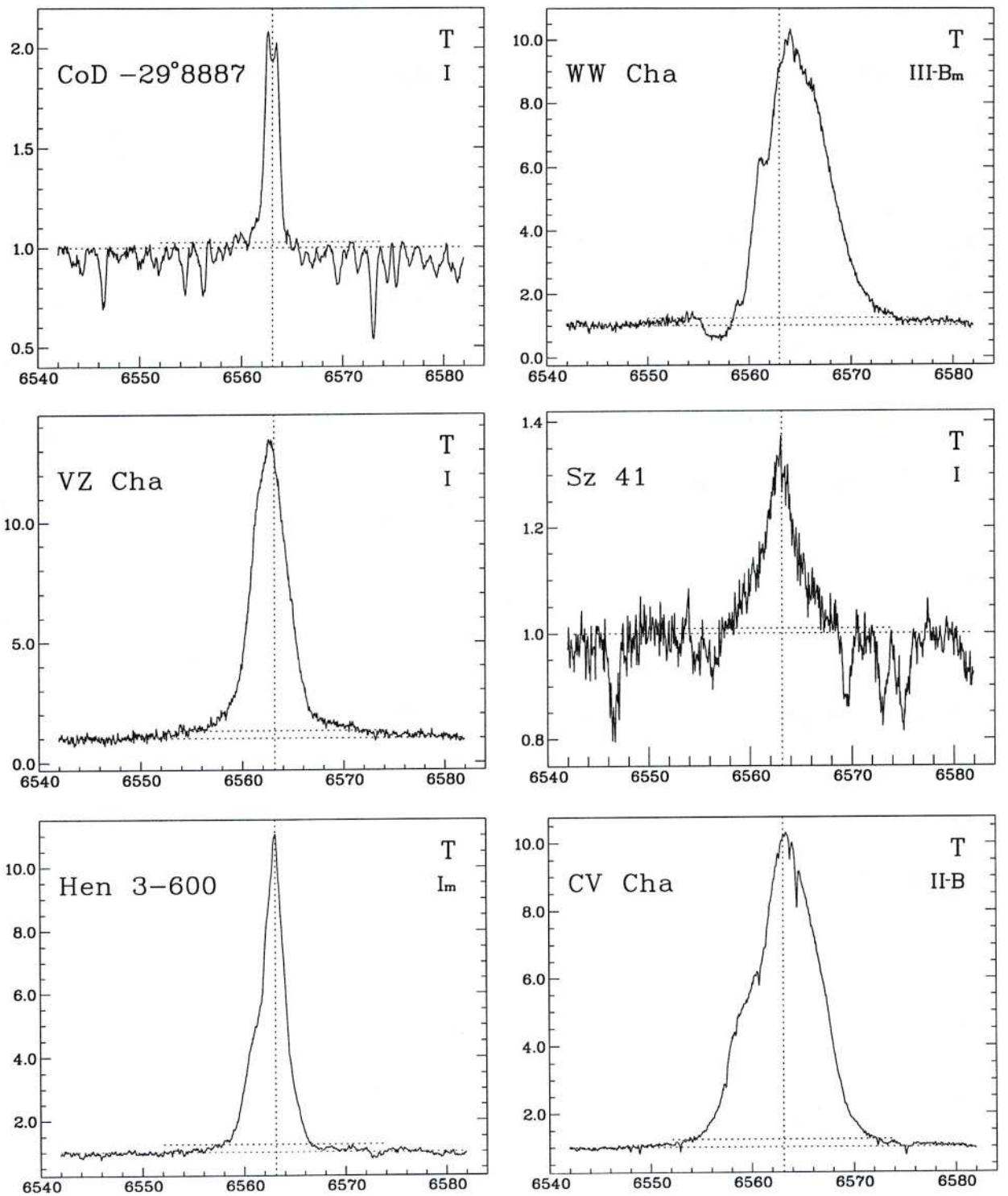

Fig. 1. continued

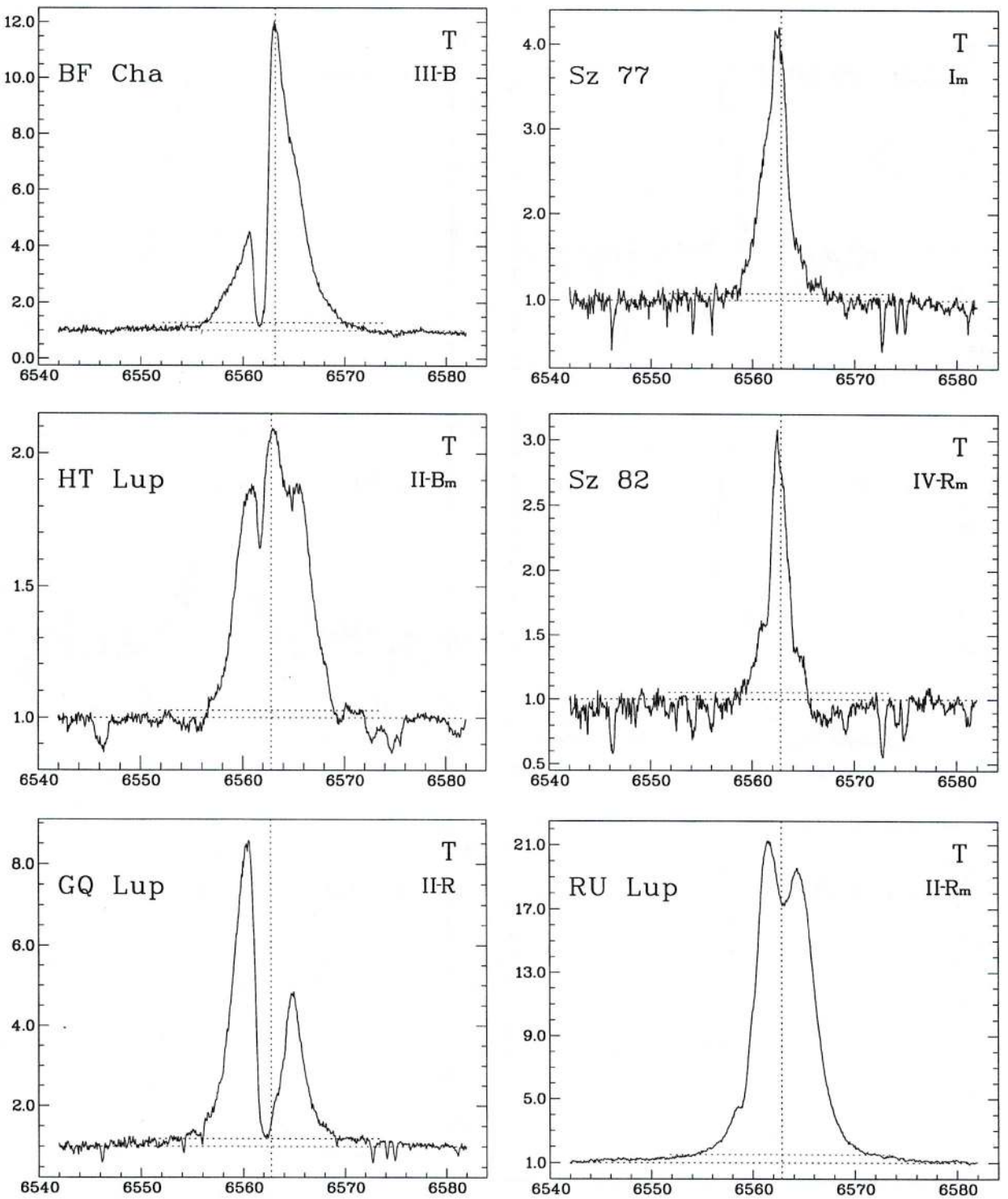

Fig. 1. continued

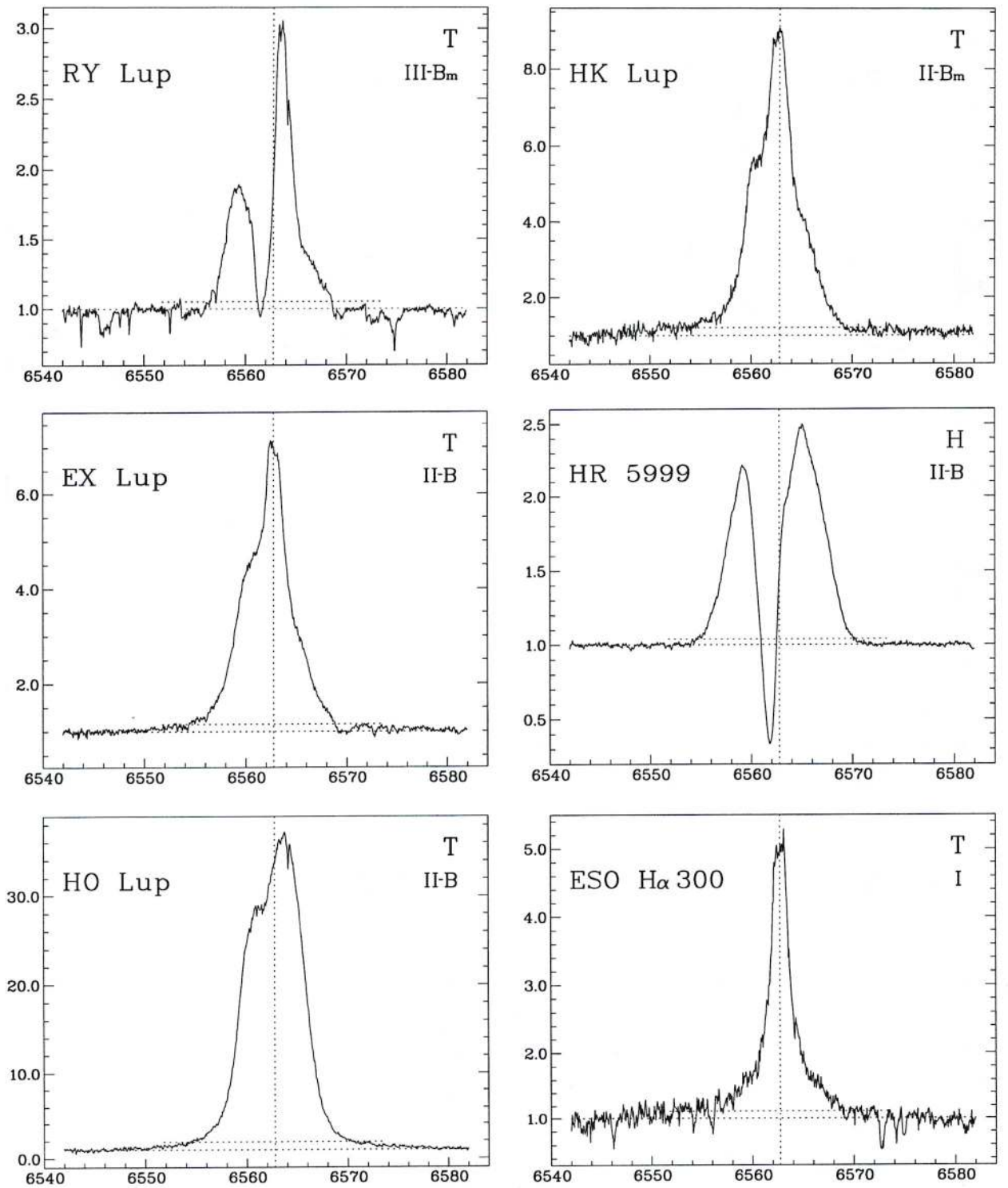

Fig. 1. continued

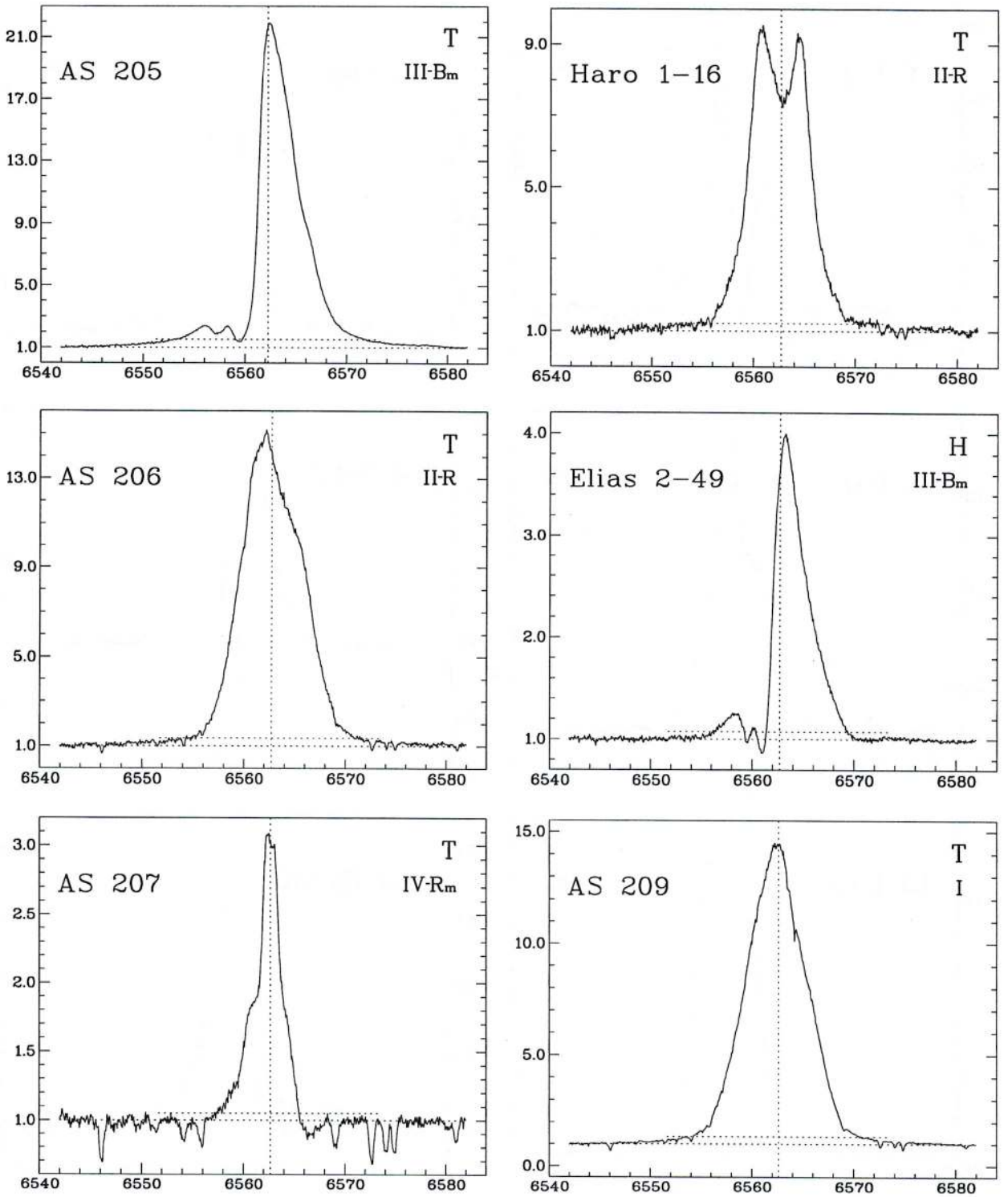

Fig. 1. continued

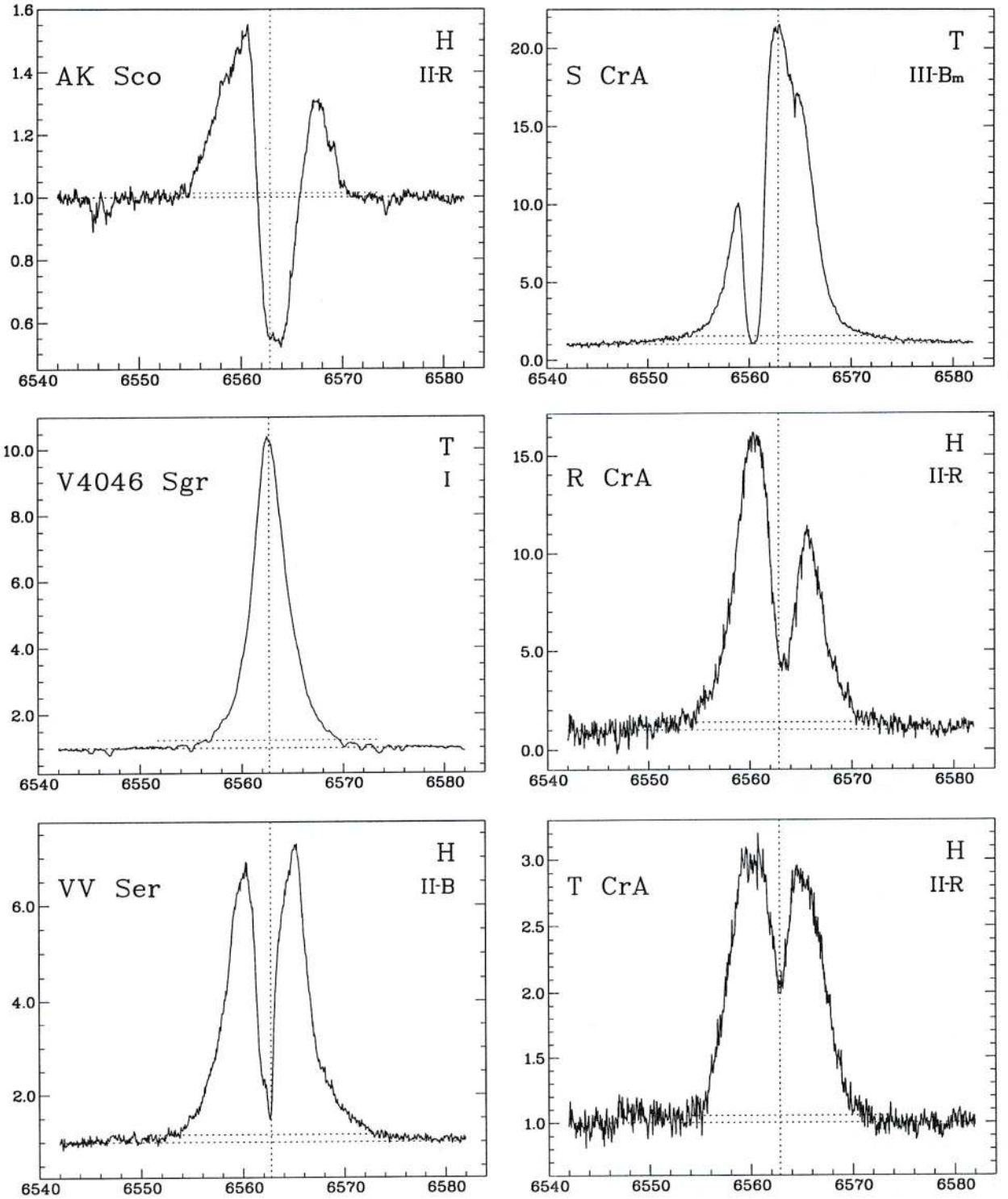

Fig. 1. continued

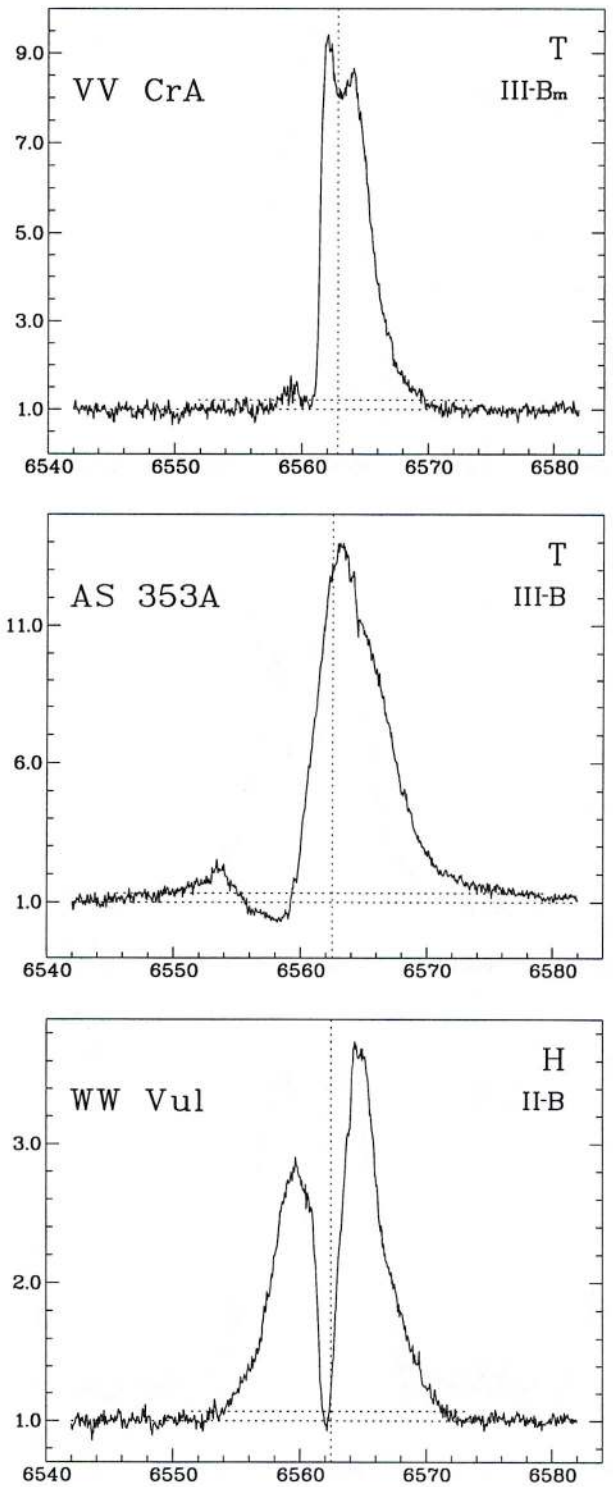

Fig. 1. continued